1521-0111/83/1/106–121$25.00
MOLECULAR PHARMACOLOGY

http://dx.doi.org/10.1124/mol.112.081802
Mol Pharmacol 83:106–121, January 2013

Activation of Group I Metabotropic Glutamate Receptors Potentiates Heteromeric Kainate Receptors

Asheebo Rojas, Jonathon Wetherington, Renee Shaw, Geidy Serrano, Sharon Swanger, and Raymond Dingledine

Department of Pharmacology, Emory University, Atlanta, Georgia

Received August 10, 2012; accepted October 11, 2012

ABSTRACT

Kainate receptors (KARs), a family of ionotropic glutamate receptors, are widely expressed in the central nervous system and are critically involved in synaptic transmission. KAR activation is influenced by metabotropic glutamate receptor (mGlu) signaling, but the underlying mechanisms are not understood. We undertook studies to examine how mGlu modulation affects activation of KARs. Confocal immunohistochemistry of rat hippocampus and cultured rat cortex revealed colocalization of the high-affinity KAR subunits with group I mGlu receptors. In hippocampal and cortical cultures, the calcium signal caused by activation of native KARs was potentiated by activation of group I mGlu receptors. In *Xenopus laevis* oocytes, activation of group I mGlu receptors potentiated heteromeric but not homomeric KAR-mediated currents, with no change in agonist potency. The potentiation of heteromeric KARs by mGlu1 activation was attenuated by GDPβS, blocked by an inhibitor of phospholipase C or the calcium chelator 1,2-bis(*o*-aminophenoxy)ethane-*N*,*N*,*N*′,*N*′-tetraacetic acid (BAPTA), prolonged by the phosphatase inhibitor okadaic acid, but unaffected by the tyrosine kinase inhibitor lavendustin A. Protein kinase C (PKC) inhibition reduced the potentiation by mGlu1 of GluK2/GluK5, and conversely, direct activation of PKC by phorbol 12-myristate,13-acetate potentiated GluK2/GluK5. Using site-directed mutagenesis, we identified three serines (Ser833, Ser836, and Ser840) within the membrane proximal region of the GluK5 C-terminal domain that, in combination, are required for mGlu1-mediated potentiation of KARs. Together, these data suggest that phosphorylation of key residues in the C-terminal domain changes the overall charge of this domain, resulting in potentiated agonist responses.

Introduction

Kainate receptors (KARs) are widely distributed throughout the central nervous system in areas such as the hippocampus, cortex, amygdala, retina, striatum, hypothalamus, cerebellum, spinal cord, and dorsal root ganglia, where they are located on both presynaptic and postsynaptic terminals and mediate synaptic transmission and synaptic plasticity (Chittajallu et al., 1996, Clarke et al., 1997, Rodriguez-Moreno et al., 1997, Bortolotto et al., 1999a, Lerma et al., 2001, Huettner, 2003, Lerma, 2003). Kainate receptors are tetrameric glutamate-gated ion channels assembled from GluK1-GluK5 subunits (Traynelis et al., 2010). The GluK1, GluK2, and GluK3 subunits (previously termed GluR5, GluR6, and GluR7) are capable of forming functional homomeric channels; however, the GluK4 and GluK5 subunits (previously termed KA1 and KA2) require coassembly with GluK1, GluK2, or GluK3 to form functional channels (Sommer et al., 1992, Egebjerg and Heinemann, 1993, Wenthold et al., 1994, Schiffer et al., 1997, Traynelis et al., 2010). In the hippocampus, kainate receptor subunits show distinct regional and subcellular localization (Bahn et al., 1994, Bureau et al., 1999, Paternain et al., 2000, Isaac et al., 2004). For example, GluK2-, GluK4-, and GluK5-containing receptors are highly expressed in the CA3 pyramidal cell layer, whereas GluK1 is barely detectable.

Metabotropic glutamate receptors (mGlu) also play critical roles in synaptic plasticity and neuronal excitability (Anwyl, 1994, Bortolotto et al., 1999b). Previous studies have

This work was supported by the National Institutes of Health National Institute of Neurologic Disorders and Stroke [Grants 5R01NS036604 and 5P30NS055077], and the National Institutes of Health National Institute on Drug Abuse [Grant 5T32DA15040].
dx.doi.org/10.1124/mol.112.081802.

ABBREVIATIONS: A841720, 9-(dimethylamino)-3-(hexahydro-1*H*-azepin-1-yl)pyrido[3′,2′:4,5]thieno[3,2-*d*]pyrimidin-4(3*H*)-one; ACPD, 1-aminocyclopentane-1,3-dicarboxylic acid; AMPA, amino-3-hydroxy-5-methyl-4-isoxazolepropionic acid; L-AP4, L-(+)-2-amino-4-phosphonobutyric acid; AMN082, *N*,*N*′-bis(diphenylmethyl)-1,2-ethanediamine]; ANOVA, analysis of variance; BAPTA, 1,2-bis(*o*-aminophenoxy)ethane-*N*,*N*,*N*′,*N*′-tetraacetic acid; CHPG, 2-chloro-5-hydroxyphenylglycine; CNQX, 6-cyano-7-nitroquinoxaline-2,3-dione; DHPG, dihydroxyphenylglycine; DMSO, dimethyl sulfoxide; GluK, kainate receptor; GYKI 52466 hydrochloride, 4-(8-methyl-9*H*-1,3-dioxolo[4,5-*h*][2,3]benzodiazepin-5-yl)-benzenamine dihydrochloride; HBSS, Hanks' balanced salt solution; KAR, kainate receptor; mGlu, metabotropic glutamate receptor; MK801, (5*S*,10*R*)-(+)-5-methyl-10,11-dihydro -5*H*-dibenzo[*a*,*d*]cyclohepten-5,10-imine maleate; MPEP, 2-methyl-6-(phenylethynyl) pyridine; NMDA, *N*-methyl-D-aspartic acid; NBQX, 2,3-dioxo-6-nitro-1,2,3,4-tetrahydrobenzo[*f*]quinoxaline-7-sulfonamide; PICK1, protein interacting with PRKCA1; PKC, protein kinase C; PMA, phorbol 12-myristate 13-acetate; Ro 320432, 3-[(8*S*)-8-[(dimethylamino)methyl]-6,7,8,9-tetrahydropyrido[1,2-*a*]indol-10-yl]-4-(1-methyl-1*H*-indol-3-yl)-1*H*-pyrrole-2,5-dione hydrochloride; SNAP-25, synaptosomal-associated protein 25; SYM2081, (2*S*,4*R*)-4-methylglutamic acid; *trans*-ACPD, (±)-1-aminocyclopentane-*trans*-1,3-dicarboxylic acid; U73122, 1-[6-[[(17β)-3-methoxyestra-1,3,5(10)-trien-17-yl]amino]hexyl]-1*H*-pyrrole-2,5-dione; U73343, 1-[6-[[(17β)-3-methoxyestra-1,3,5(10)-trien-17-yl]amino]hexyl]-2,5-pyrrolidinedione; VDCC, voltage-dependent Ca^{2+} channel.

demonstrated altered function and/or distribution of both amino-3-hydroxy-5-methyl-4-isoxazolepropionic acid (AMPA) and NMDA receptors after activation of group I mGlu receptors (Anwyl, 1999). For example, activation of group I mGlu receptors potentiates NMDA responses in hippocampal slices and in *Xenopus laevis* oocytes injected with rat brain mRNA (Aniksztejn et al., 1992, Kelso et al., 1992, Harvey and Collingridge, 1993). Cho et al. (2003) reported that activation of a G_q-coupled group I metabotropic glutamate receptor (likely mGlu5) potentiates GluK1-mediated KAR responses in neurons from the perirhinal cortex in a PKC-dependent manner. Of interest, PKC phosphorylates the C terminus of GluK1 and GluK2 in vitro, which has been proposed to increase the contribution of KARs to the synaptic response (Hirbec et al., 2003, Nasu-Nishimura et al., 2010, Konopacki et al., 2011, Chamberlain et al., 2012). GluK2 is also phosphorylated by the cAMP-dependent protein kinase A (Raymond et al., 1993, Wang et al., 1993, Raymond et al., 1994, Traynelis and Wahl, 1997, Kornreich et al., 2007). In experiments using *X. laevis* oocytes and recombinant KARs, inclusion of high-affinity KAR subunits (GluK4 or GluK5) into heteromeric assemblies with GluK2 confers different biophysical, pharmacological, and functional properties on the resulting channels. Here, we ask the following questions: does incorporation of the high-affinity kainate receptor subunits into heteromeric complexes with GluK2 bestow regulation by group I mGlu receptors and PKC signaling? Which protein domains and amino acid residues are involved? To address these questions, we combined confocal imaging, cellular Ca^{2+} signal assays, and functional studies of coexpressed recombinant mGlu receptors and KARs. We conclude that phospholipase C, Ca^{2+}, and PKC are in a pathway that converges on critical residues within the C-terminal domain of the GluK5 subunit. This receptor cross-talk between mGlu receptors and heteromeric KARs adds a new dimension to KAR function and is likely to be one of the mechanisms underlying the activity-dependent modulation of KARs in synaptic plasticity and neuronal excitability.

Materials and Methods

Molecular Biology. Rat GluK2(R) (GenBank NM_019309.2) in the pSGEM vector was a generous gift from Dr. Mark Mayer (National Institutes of Health, Bethesda, MD). Plasmids encoding rat GluK1 (GenBank NM_001111117.1), GluK4 (GenBank U08257), and GluK5 (GenBank NM_031508) were generously provided by Dr. Stephen Heinemann (Salk Institute, San Diego, CA). Rat GluN1 (GenBank NM_017010) and GluN2A (GenBank D13211) were generously provided by Dr. Shigetada Nakanishi (Kyoto University, Kyoto, Japan). Rat mGlu1 (GenBank X57569), mGlu5 (GenBank D10891), and mGlu7 (GenBank D16817), all in pBluescript, were generously provided by Dr. Jeffrey Conn (Vanderbilt University Medical Center, Nashville, TN). Mutations were generated using the QuikChange site-directed mutagenesis kit (Stratagene, La Jolla, CA) according to the manufacturer's protocol. All mutants were subcloned back into the original receptor vector (i.e., pGEM, pSGEM, or pCMVTNT for GluK5) using the SphI and XbaI sites. Correct constructions and mutations were confirmed by DNA sequencing. All cRNAs were transcribed in vitro from linearized cDNA templates using the mMessage mMachine kit (Ambion, Austin, TX) and purified for injection into oocytes.

Oocyte Preparation and Injection. All procedures and experiments conformed to the guidelines of the Animal Care and Use Committee of Emory University. *X. laevis* oocytes were prepared and injected as described previously (Kawajiri and Dingledine, 1993). In brief, stage V-VI oocytes were removed from frogs that had been anesthetized in water containing 0.156% tricaine. After treatment with type IV collagenase (Worthington Biochemical, Lakewood, NJ; 1.7 mg/ml for 45–120 min) in a calcium-free Barth's solution, oocytes rested overnight and were then injected with 50-100 ng of mRNA transcribed from linearized constructs in the pCMVTNT, pSGEM, or pBluescript vectors. For the expression of heteromeric receptors, mRNAs were injected at a 1:3 weight ratio (GluK2/GluK4, GluK2/GluK5, and GluN1/GluN2A) with or without an equal weight of mGlu1, mGlu5, or mGlu7 mRNA. Before electrophysiological recording, injected oocytes were maintained at 18°C for 3–10 days in Barth's solution containing 88 mM NaCl, 2.4 mM $NaHCO_3$, 1 mM KCl, 0.33 mM $Ca(NO_3)_2$, 0.91 mM $CaCl_2$, 0.82 mM $MgSO_4$, and 5 mM Tris/HCl, pH 7.4, and supplemented with gentamycin (100 μg/ml), penicillin (10 U/ml), and streptomycin (10 μg/ml).

Electrophysiology. Two-electrode voltage-clamp recordings were performed at room temperature (23–25°C) from cells continually perfused in a standard frog Ringer's solution containing 90 mM NaCl, 1 mM KCl, 15 mM HEPES, and 0.5 mM $BaCl_2$, pH, 7.4. Recording pipettes were filled with 3 M KCl. GluK1 and GluK2 homomeric receptors were activated by bath application of domoate (3 μM). GluK2/GluK4 and GluK2/GluK5 receptors were activated by bath application of AMPA (1–300 μM) to avoid the activation of homomeric KAR. NMDA receptors were activated by bath application of NMDA (100 μM) and glycine (10 μM) (Kleckner and Dingledine, 1988). Currents were elicited from a holding potential of −60 mV unless otherwise specified. Current records were digitized at 1 kHz with a Digidata 1200 analog to digital converter (Axon Instruments, Foster City, CA) under the control of pClamp 8 acquisition software (Molecular Devices, Sunnyvale, CA) and stored on a computer disk for later analysis. Application of each agonist produced a stable, rapidly increasing, and nondesensitizing or weakly desensitizing current in the majority of oocytes. Results from oocytes in which the agonist-induced current was not stable under baseline conditions or the baseline holding current at the beginning and end of the experiment drifted by more than 10% were discarded.

Immunohistochemistry. All experimental procedures were performed in accordance with the guidelines for the Care and Use of Laboratory Animals by Emory University. Male Sprague-Dawley rats (200–250 g) were deeply anesthetized by inhalation with isoflurane and perfused transcardially with 0.9% saline, followed by 4% (wt/vol) paraformaldehyde in 0.1 M phosphate-buffered saline (PBS; pH, 7.4). The brains were rapidly dissected, post-fixed in the same solution at 4°C overnight, and then transferred to 30% (w/v) sucrose in phosphate buffer at 4°C until they sank. The brains were then mounted onto a tissue-cutting block and frozen in optimum cutting temperature compound (VWR, West Chester, PA). Coronal or sagittal sections (40 μm) were cut using a cryostat CM 1850 (Leica, Wetzlar, Germany) and placed in 0.05 M Tris-buffered saline (TBS; free-floating). The sections were then separated for fluorescence and diaminobenzidine (DAB) immunostaining. For DAB staining, the sections were washed five times with TBS for 5 minutes each and then treated with 0.5% H_2O_2 for 30 minutes. The sections were washed to remove H_2O_2 and then blocked with TBS containing 1% bovine serum albumin (BSA), 10% normal serum (NS), and 0.3% Triton X-100 at 25°C for 45 minutes, to reduce nonspecific immunostaining. The sections were then incubated in the primary antibodies (goat anti-GluK4, 1:50 and goat anti-GluK5, 1:50; Santa Cruz Biotechnology, Santa Cruz, CA) diluted in antibody dilution solution (ADS) containing 0.1% gelatin and 0.3% Triton X-100 in TBS at 4°C for 48 hours. After washing three times with ADS, the sections were incubated with a donkey anti-goat HRP-conjugated secondary antibody (Jackson ImmunoResearch Laboratories, West Grove, PA) diluted to 1:200 in ADS for 4 hours at 25°C. The sections were washed with TBS and exposed to DAB (DAB enhancement kit; Sigma-Aldrich, St. Louis, MO). The floating sections were subsequently mounted onto clean slides and allowed to dry. After drying, the sections were dehydrated by exposure to

increasing concentrations of ethanol, made transparent with xylenes and then coverslipped in the presence of permount.

For fluorescence immunohistochemistry, the sections were washed three times with 1× PBS, blocked for 45 minutes in PBS containing 1% BSA, and incubated in primary antibodies (goat anti-GluK4, goat anti-GluK5; Santa Cruz Biotechnology; rabbit anti-mGlu1, rabbit anti-mGlu5; Millipore, Temecula, CA; all at 1:50) as described above. After washing three times with ADS, the sections were incubated with the appropriate Alexa Fluor fluorophore-conjugated secondary antibodies (Alexa Fluor donkey anti-goat 488, Alexa Fluor chicken anti-rabbit 594; Molecular Probes, Eugene, OR) diluted to 1:200 in ADS for 4 hours at 25°C. The sections were washed three times with PBS and then incubated with the blue-fluorescent Hoechst 33342 dye (Molecular Probes) diluted 1:5000 in ADS for 4 hours at 25°C. The sections were again washed with PBS, mounted onto slides, allowed to dry, and coverslipped with Fluoro Gel mount. The DAB and fluorescence reactions were visualized using an Axio Observer A1 fluorescence microscope (Zeiss, Oberkochen, Germany). Pictures were taken using the AxioVision AC 4.1 software (Zeiss). Fluorescence images were also taken with a LSM 510 Meta Zeiss laser scanning confocal microscope coupled to a Zeiss AxioObserver Z1 at one focal plane (Carl Zeiss GmbH, Jena, Germany). In control experiments, the sections were treated in a similar manner, except that the primary antibodies were omitted. All negative control sections showed no staining (data not shown). The DAB KAR staining profiles in the hippocampus using the GluK4 and GluK5 polyclonal antibodies purchased from Santa Cruz Biotechnology were very similar to that found by Darstein et al. (2003), who demonstrated specificity of their GluK5 antibody in a Western blot using brains taken from GluK5 knockout mice.

Hippocampal and Cortical Culture and Immunocytochemistry. The entire hippocampus and cortex were isolated separately from embryonic day-16–18 embryos of timed-pregnant Sprague-Dawley rats. The tissue was dissociated after papain exposure, and the cells were plated as described by Jiang et al. (2010). In brief, cells were plated onto poly-D-lysine–coated 96-well plates (black with clear bottom) at a density of 150,000 cells/well in Neurobasal medium supplemented with B27 and 5% fetal bovine serum (Invitrogen, Carlsbad, CA). The cultures were incubated at 37°C in 95% air/5% CO_2, and half of the culture medium was replaced every 3–4 days with serum-free medium. After 5–10 days in culture, the cortical cells were fixed with 4% paraformaldehyde in PBS and then permeabilized with 0.2% Triton X-100. After incubation in blocking buffer made with PBS (containing 1% BSA, 10% normal serum, and 0.3% Triton X-100) at 25°C for 3 hours, the cells were incubated with the primary antibodies (goat anti-GluK4, goat anti-GluK5, Santa Cruz Biotechnology; rabbit anti-mGlu1, rabbit anti-mGlu5, Millipore, Temecula, CA; mouse anti-synapsin I; BD Biosciences, Franklin Lakes, NJ; all at 1:50) overnight, followed by staining with the appropriate Alexa Fluor fluorophore conjugated secondary antibodies (Alexa Fluor chicken anti-rabbit 594, Alexa Fluor donkey anti-goat 488, Alexa Fluor goat anti-mouse 594; Molecular Probes, OR; diluted at 1:200). The cells were then incubated with the blue-fluorescent Hoechst 33342 dye (Molecular Probes) for 4 hours at 25°C. Fluorescence images were taken with a LSM 510 Zeiss confocal microscope (Carl Zeiss GmbH).

Quantification of Colocalization. Colocalization quantification was performed on representative single confocal overlay (GluK, green; mGlu, red) images taken using a 20× and a 40× objective lens from a single confocal plane. After double-labeling immunohistochemistry, two channels representing the two protein stains (i.e., red and green) were used for the colocalization analysis. Quantification of colocalized signal intensities in each optical section was analyzed with the Coloc module of the IMARIS image analysis software (IMARIS 6.4.0; Bitplane, Zurich, Switzerland). A region of interest (ROI) in the hippocampal sections was chosen as an oval drawing outlying a specific area (i.e., stratum radiatum or stratum lucidum) in the CA3 region of the hippocampus. The entire image was selected as the ROI for the cell culture colocalization. Multiple images were analyzed for colocalization quantification from independent immunostains. Background was normalized by selective determination of the intensity threshold in both channels with use of the algorithm in the Coloc software. Pixel codistribution was calculated for green and red staining patterns throughout the ROI. Colocalized pixels were displayed in a white mask overlapping the fluorescence channels over the image. The results were expressed as a Mander's correlation coefficient for pixel intensity correlation between the green (GluK4, GluK5, synapsin I) and red (mGlu1, mGlu5) channels. An ROI was selected for analysis if it contained greater than 24,000 voxels. Multiple ROIs within the hippocampal area were selected and analyzed at 20× magnification. At this lower magnification, the ROIs were averaged and plotted as mean ± S.E.M. Higher magnification images (taken using a 40× objective lens) were also analyzed for colocalization quantification, because the pixel overlap was not clear at the lower magnification and there was pronounced punctuate staining in the CA3 area at the higher magnification. To avoid overlapping and to obtain enough pixels for the analysis a single region of interest was selected for the 40× confocal images. For the negative control sections, the staining procedure was similar except the primary antibodies were omitted. The positive control was a hippocampal immunostain in which GluK5 was labeled with both 488- and 594-conjugated secondary antibodies. The Mander's correlation coefficient threshold (the cutoff) was determined by the negative control of the double-labeling immunohistochemistry.

Measurement of $[Ca^{2+}]_i$ in Rat Hippocampal and Cortical Cultures Using a Ca^{2+}-Sensitive Dye. Rat neurons isolated from the entire hippocampus or cortex were plated onto poly-D-lysine–coated 96-well plates as described above. After 5 days in culture, the level of intracellular calcium was assayed using the Fluo-4 No Wash calcium assay kit according to the manufacturer's protocol (Invitrogen, Carlsbad, CA). In brief, the neuronal culture medium was removed and replaced with a calcium assay buffer (CAB) containing 1× HBSS, 20 mM HEPES, 2.5 mM probenacid, and Fluo4-NW dye mix (pH 7.4; Invitrogen, Carlsbad, CA). The cells were then incubated for 45 minutes at 37°C for dye loading and then 15 minutes at 25°C. To isolate calcium signals mediated by heteromeric KARs, AMPA was used as an agonist, and 10 μM MK801, 100 μM D-(-)-2-amino-5-phosphonopentanoic acid (D-AP5), 100 μM bicuculline, and 100 μM GYKI 52466 were added to the CAB before dye loading. The antagonist MPEP or PKC inhibitor Ro 320432 [3-[(8*S*)-8-[(dimethylamino) methyl]-6,7,8,9-tetrahydropyrido[1,2-*a*]indol-10-yl]-4-(1-methyl-1*H*-indol-3-yl)-1*H*-pyrrole-2,5-dione hydrochloride] was applied to the CAB and loaded onto one-half of the 96-well plates. The calcium fluorescence measurement was performed at 25°C. CAB with or without dihydroxyphenylglycine (DHPG) was added (25 μl, 5× final concentration of 50 μM) after 60 seconds of recording with a FLEXStation II benchtop scanning fluorometer (Molecular Devices); then, the glutamate receptor agonist AMPA (25 μl, 6×) was added at 180 seconds. Phorbol 12-myristate 13-acetate (PMA) exposure was performed in the same manner as DHPG. Fluorescence plate reading continued for a total of 400 seconds with use of an excitation of 485 nM, an emission of 538 nM, and a cutoff of 530 nM. Agonist and vehicle were added at a speed of 26 μl/s. The data were recorded using SoftMax Pro software (Molecular Devices).

Chemicals and Reagents. Domoic acid, *RS*-α-amino-3-hydroxy-5-methyl-4-isoxazolepropionic acid, (±)-1-aminocyclopentane-*trans*-1, 3-dicarboxylic acid (*trans*-ACPD), *RS*-DHPG, (*RS*)-2-chloro-5-hydroxyphenylglycine (CHPG), NMDA, (2*S*,2′*R*,3′*R*)-2-(2′,3′-dicarboxycyclopropyl)glycine, 9-(dimethylamino)-3-(hexahydro-1*H*-azepin-1-yl) pyrido[3′,2′:4,5]thieno[3,2-*d*]pyrimidin-4(3*H*)-one (A841720), 4-(8-methyl-9*H*-1,3-dioxolo[4,5-*h*][2,3]benzodiazepin-5-yl)-benzenamine dihydrochloride (GYKI 52466 hydrochloride), bicuculline methochloride, thapsigargin, MK801 [(5*S*,10*R*)-(+)-5-methyl-10,11-dihydro-5*H*-dibenzo[*a*,*d*]cyclohepten-5,10-imine maleate], ionomycin, CNQX, NBQX, SYM2081 [(2*S*,4*R*)-4-methylglutamic acid], and U73122 [1-[6-[[(17β)-3-methoxyestra-1,3,5(10)-trien-17-yl]amino]hexyl]-1*H*-pyrrole-2,5-dione] were purchased from Tocris Bioscience (Ellisville, MO). Protein kinase inhibitors (genistein, lavendustin A, lavendustin B, staurosporine) were purchased

from Calbiochem (La Jolla, CA). Thymeleatoxin, PMA, 4α-PMA, BAPTA, GDPβS, and KCl salt were all purchased from Sigma-Aldrich. Okadaic acid was from LC Laboratories/Alexis (Switzerland). U73343 [1-[6-[[(17β)-3-methoxyestra-1,3,5(10)-trien-17-yl]amino]hexyl]-2,5-pyrrolidinedione] and Ro 320432 were purchased from BioMol (Plymouth Meeting, PA). D-AP5 was purchased from Ascent Scientific (Princeton, NJ). Molecular biology reagents and restriction enzymes were purchased from New England Biolabs (Ipswich, MA) and Promega (Madison, WI). A841720, U73122, U73343, genistein, lavendustin A and B, staurosporine, Ro 320432, thymeleatoxin, PMA, 4α-PMA, thapsigargin, CNQX, NBQX, and okadaic acid were dissolved in dimethyl sulfoxide (DMSO) as stocks and mixed with the recording solution, reaching a final concentration as indicated in the results. The final DMSO concentration was $\leq$0.2%, which had no effect on responses. Other chemicals were dissolved in doubly distilled water or experimental solutions.

Data Analysis. Data analysis for intracellular calcium detection was performed using Microsoft Excel and Origin (Microcal Software, Northampton, MA). Data analysis for oocyte recording was performed using pClamp and Clampfit 9 (Axon Instruments, Foster City, CA) and Origin. Data are presented as means $\pm$ S.E.M. Student's t test or one-way analysis of variance (ANOVA) with Bonferroni-corrected or Dunnett's comparison of selected means was performed to examine differences of chemical effects in the absence versus the presence of the chemical. The differences were considered to be statistically significant if $P \leq 0.05$.

Results

Colocalization of KAR Subunits and Group I mGlu Receptors in Rat Hippocampus. If direct functional cross-talk between KARs and mGlu receptors exists, these receptors should be expressed in close proximity. DAB and fluorescent immunohistochemistry were performed on fixed 40-μm rat hippocampal sections to determine whether KARs and mGlu receptors are coexpressed in the hippocampus. GuK5 and mGlu5 are shown in Fig. 1, B and D–F. The expression pattern of GluK5 in Fig. 1A closely mimicked that found by Darstein et al., 2003. Immunostains were also obtained for GluK4, GluK5, mGlu1, and mGlu5 in the hippocampus of two or more adult male Sprague-Dawley rats with distributions consistent with previous reports (Berthele et al., 1998, Ferraguti et al., 1998, Darstein et al., 2003, Besheer and Hodge, 2005, Simonyi et al., 2005). All four antigens (GluK4, GluK5, mGlu1, and mGlu5) were labeled by both DAB and fluorescent secondary antibodies. Pronounced staining of all four antigens was detected in the CA3 region of the hippocampus, and thus, we focused on this region for the determination of colocalization. Double-labeling immunohistochemistry on multiple coronal and sagittal hippocampal sections (40 μm) revealed colocalization of both GluK5 and mGlu5 in CA3. Punctate staining was particularly observed in the stratum radiatum of CA3 at higher magnifications using a laser confocal microscope (Fig. 1, D and E). The immunostains for GluK5 and mGlu5 showed intense punctate overlapping positive staining in the stratum radiatum, suggesting that these two proteins are colocalized (Fig. 1, B and F). Quantification of colocalization was performed on single confocal images with use of the Imaris image analysis software. At a lower magnification (20×), multiple ROIs were selected and averaged. The Mander's correlation coefficients of colocalization for the kainate receptors and group I metabotropic receptors obtained by selecting multiple ROIs were consistent with the higher magnification images that showed pronounce punctuate staining (taken using a 40×/1.3 oil objective lens) (Fig. 1C). The analysis revealed a significant Mander's coefficient (Manders et al., 1993) of colocalization that was above background for GluK5 paired with mGlu5 in the stratum radiatum but not GluK4 paired with mGlu5 in the stratum lucidum, nor GluK4 paired with mGlu1 in either region, confirming that the colocalization is not random (Fig. 1C). A Mander's coefficient above threshold was also observed for mGlu1 and GluK5 in the stratum lucidum, suggesting colocalization of the two subunits in the mossy fibers (Fig. 1C, inset). Although the mGlu5 signal was extensive in the stratum radiatum (Fig. 1E), there was no colocalization of mGlu5 with GluK4 in this region, because quantification of colocalization revealed a very low Mander's coefficient. Likewise, the absence of colocalized pixels of GluK5 with mGlu5 in the stratum lucidum, although both were expressed in the same dendrites, confirms the specificity of this measure. This represents the first evidence of colocalization of the high-affinity KAR subunits with group I mGlu receptors in the same subcellular compartments of hippocampal neurons. In addition to the expression of GluK4 and GluK5 in the stratum lucidum, we also detected above background expression of GluK5 in the stratum radiatum, confirming a previous study (Darstein et al., 2003).

Activation of Group I mGlu Receptors Potentiates KAR in Rat Hippocampal and Cortical Cultures. The ion conduction pathway formed by KARs is permeable to calcium, in addition to sodium and potassium, although the calcium permeability is entirely dependent on RNA editing of GluK2 transcripts. Knowing this, we asked the following questions: does KAR activation in primary neuronal cultures lead to a detectable change in intracellular Ca^{2+}? If so, is the KAR Ca^{2+} signal potentiated by activation of group I mGlu receptors? To address these questions, we measured intracellular Ca^{2+} in rat hippocampal and cortical cultures using a fluorescent Ca^{2+} sensing dye (Fluo-4) and a FLEXStation 96-well fluorometer. Because of a limited ability to obtain sufficient hippocampal neurons from rat pups, we performed most of these experiments using cortical cultures. Immunocytochemistry showed the presence of all four antigens (GluK4, GluK5, mGlu1, and mGlu5) in cortical neurons. Visual overlapping of the double labeling and quantification of colocalization on representative single confocal images (100×/1.3 oil) with use of the Imaris image analysis software revealed colocalization of the GluK4 and GluK5 subunits with group I mGlu receptors in rat cultured cortical neurons (Fig. 2).

First, the features and limitations of the Ca^{2+} assay were determined. After baseline Ca^{2+} stabilization in the cortical cultures, bath application of HBSS had no significant effect on the calcium signal, but the calcium ionophore ionomycin (100 μM) rapidly increased the fluorescent counts, which remained elevated for the remainder of the reading time (Fig. 3A). Thapsigargin (5 μM; a Ca^{2+}-ATPase inhibitor) when applied in the same manner as ionomycin caused a smaller and slower increase in the fluorescent counts (Fig. 3A). Although these two compounds led to an increase in cytosolic Ca^{2+}, their modes of action are quite different and show that we could detect changes in intracellular Ca^{2+} via different mechanisms in cultured rat cortical neurons. In the presence of NMDA, AMPA, and $GABA_A$ receptor blockers (10 μM MK801 plus 100 μM D-AP5, 100 μM GYKI 52466, and 100 μM bicuculline,

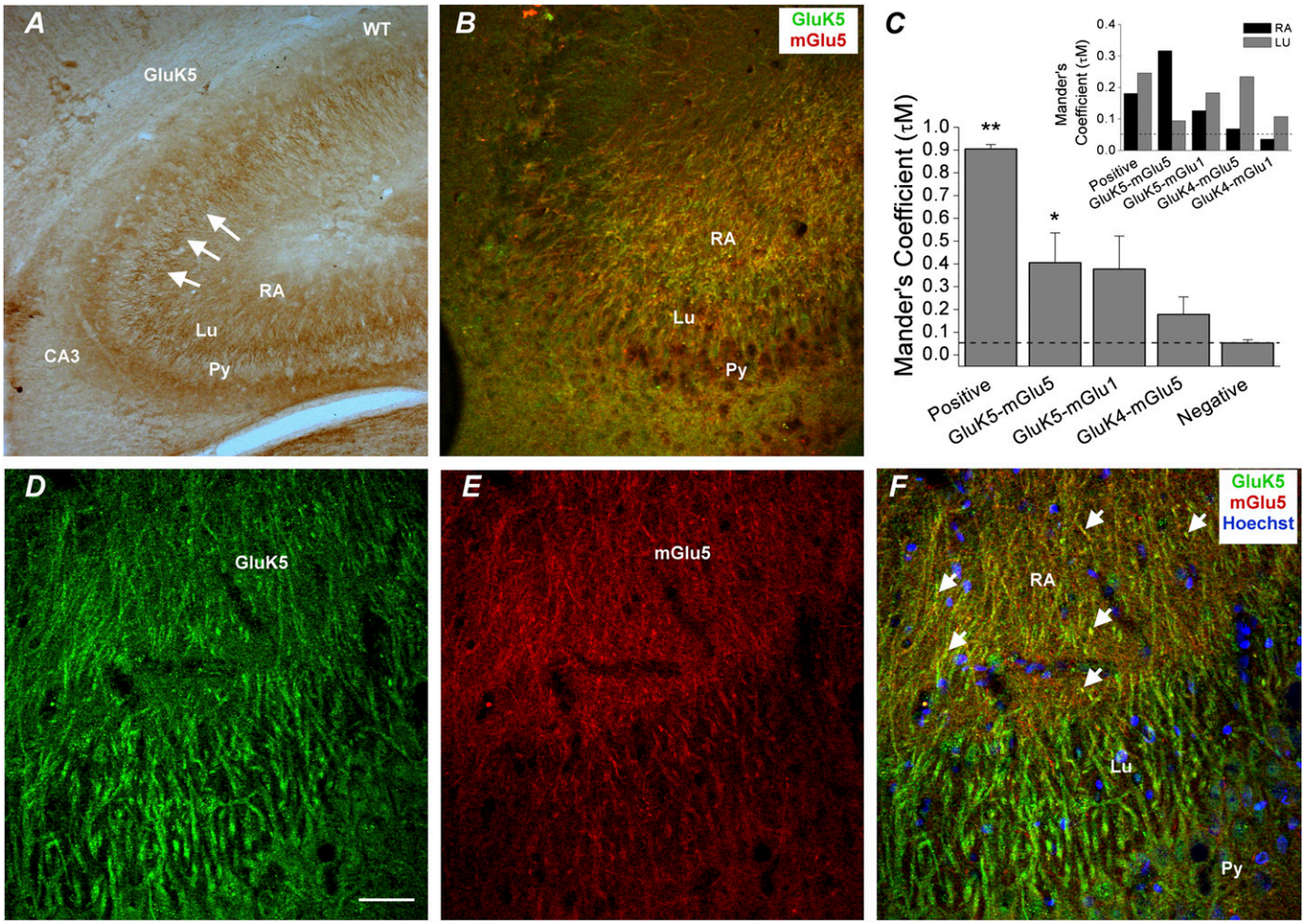

Fig. 1. Colocalization of KAR subunits and group I mGlu subunits in the rat hippocampus. DAB and fluorescent immunohistochemistry was performed on 40-μm rat hippocampal sections. (A) positive GluK5 immunoperoxidase staining in the CA3 region of the hippocampus in wild-type male Sprague-dawley rats. The arrows indicate examples of positive staining in the stratum lucidum. (B) an image taken with a 20× objective lens using a laser confocal microscope. Strong fluorescent staining for GluK5 and mGlu5 is seen in the CA3 region of the hippocampus. (C) quantification of the colocalization of the KAR subunits and the group I mGlu subunits in the stratum radiatum. Plotted is the mean ± S.E.M. from multiple ROIs with an $n \geq 4$. A significantly higher Mander's coefficient was found for GluK5-mGlu5, compared with the negative control (*$P < 0.05$, **$P < 0.01$; nne-way ANOVA with selected Dunnett's posttests). The insert is the quantification of the colocalization of the KAR subunits and the group I mGlu subunits in the stratum radiatum and stratum lucidum representing one ROI from images taken at 40×, similar to the ones in D–F. The dashed line at 0.1 represents the Mander's coefficient threshold cutoff for positive labeling as defined by the negative control. Positive designates a positive control in which GluK5 is labeled with both 488 and 594 conjugated secondary antibodies. Images in D–F were taken with a 40×/1.3 oil objective lens using a laser confocal microscope. Strong fluorescent staining for GluK5 and mGlu5 (D and E) is seen in the CA3 region of the hippocampus. (F) overlap of the GluK5 and mGlu5 immunostains. The overlapping confocal image more clearly shows the co-localization of the two subunits. The arrows indicate examples of positive colocalization. Hoechst staining revealed the nuclei of the CA3 cell layer. Lu, stratum lucidum; Py, stratum pyramidale; RA, stratum radiatum. Scale bar = 40 μm.

respectively) to isolate KARs pharmacologically, bath application of AMPA (50 μM) rapidly increased cytosolic Ca^{2+} in cortical cultures (Fig. 3B). AMPA was used at 50 μM as this concentration produced large baseline currents and was near the maximally effective concentration for rat heteromeric GluK2/GluK5 expressed in *X. laevis* oocytes (Fig. 4D; see also Mott et al., 2010).

After group I mGlu activation by DHPG (50 μM), the KAR-dependent increase in cytosolic Ca^{2+} was potentiated in cortical cultures by 134 ± 5.4% ($P < 0.05$, *t* test; $n = 19$), compared with vehicle application (Fig. 3, B and C). Likewise, there was a strong trend toward potentiation by 50 μM DHPG in the less dense hippocampal cultures (134 ± 10.9%; $n = 4$), compared with vehicle application. Potentiation of the AMPA response in cortical cultures was blocked by pretreatment with 4 μM MPEP (an mGlu5 antagonist; 98 ± 9.7% of control; $n = 6$] and by the protein kinase C inhibitor Ro 320432 (4 μM; 114 ± 16.2% of control; $n = 6$] (Fig. 3, B and C). Prior exposure to MPEP did not significantly affect the baseline calcium signal. Moreover, activation of PKC by PMA (50 nM) also potentiated the KAR -dependent increase in cytosolic Ca^{2+} in cortical cultures by 153 ± 16.4% of control ($P < 0.05$, *t* test; $n = 11$).

This AMPA-mediated increase in intracellular Ca^{2+} in the presence of a cocktail of ionotropic receptor blockers is consistent with activation of heteromeric KARs, because AMPA is a selective agonist of heteromeric but not homomeric KARs (Bettler and Mulle, 1995, Lerma et al., 2001, Traynelis et al., 2010). The AMPA-induced increase in intracellular calcium is attributed to KARs for the following reasons. First,

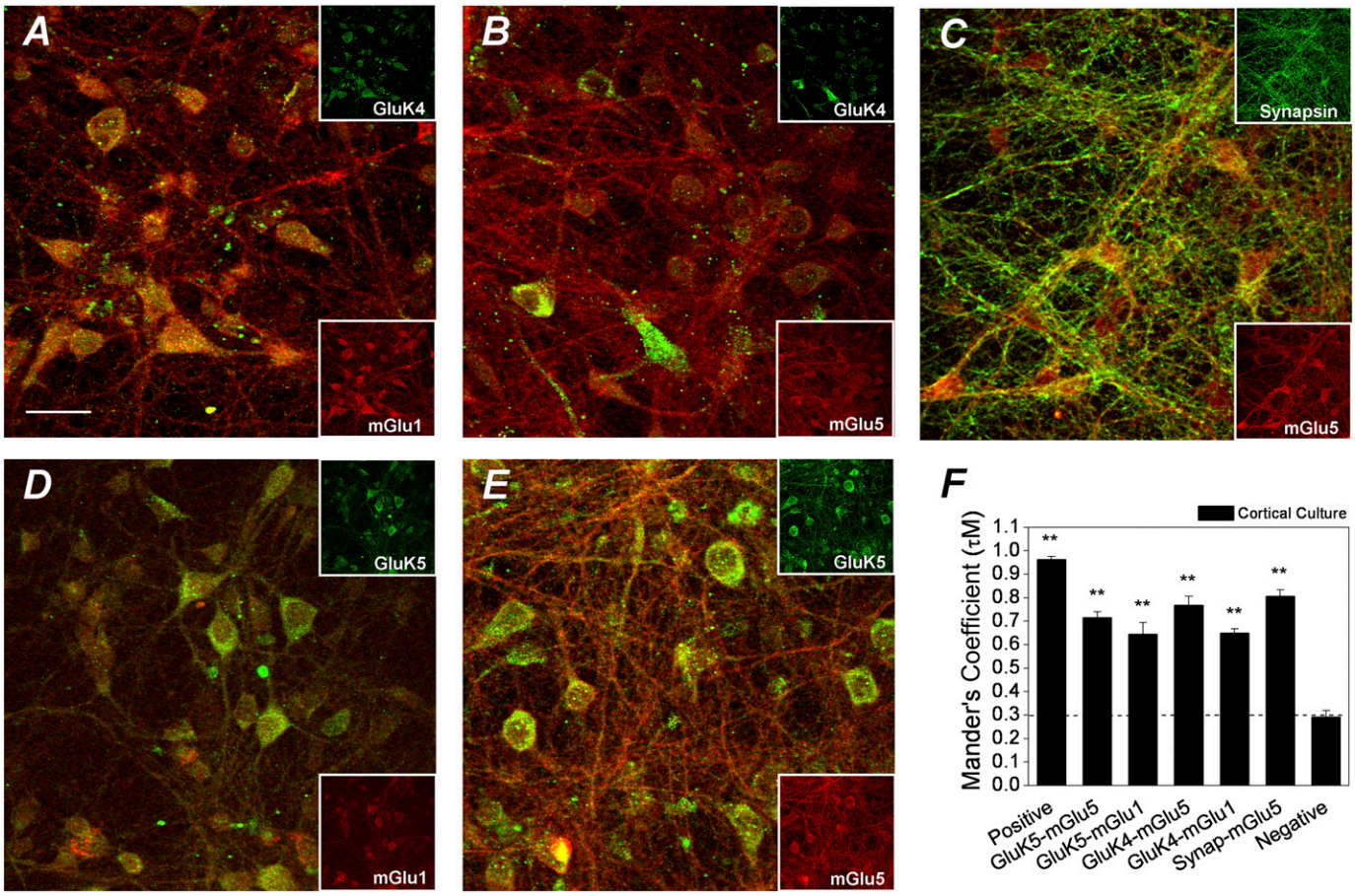

Fig. 2. Colocalization of KAR subunits and group I mGlu subunits in rat cortical cultures. Immunocytochemistry was performed on rat cortical cultures. Images were taken with a 100×/1.3 oil objective lens using a laser confocal microscope. Positive fluorescent staining was observed for mGlu1 (A and D), mGlu5 (B, C, and E), GluK4 (A and B), and GluK5 (D and E). The high magnification overlapping confocal images (A, B, D, and E) more clearly show the colocalization of the GluK and mGlu subunits. (C) overlap of synapsin and mGlu5 immunostains in the dendrites of the cortical neurons. ***F***, Quantification of the colocalization of the KAR subunits and the group I mGlu subunits in the cortical cultures ($n \geq 3$). Positive designates a positive control in which GluK5 and synapsin are stained with 594 and 488 conjugated secondary antibodies, respectively. Negative designates a negative control in which the primary antibodies are omitted. Only background staining was seen in such cultures exposed to the secondary antibodies only (data not shown) (Alexa Fluor 488 and Alexa Fluor 594). The dashed line at 0.3 represents the Mander's coefficient threshold cutoff for background labeling as defined by the negative control. All the colocalization pairs showed a significantly higher Mander's coefficient, compared with the negative control (**$P <$ 0.01; one-way ANOVA with selected Dunnett's post-tests). The bar = 20 μm.

the signal was increased by bath application of the KAR potentiator concanavalin A (a lectin from *Canavalia ensiformis*) in a dose-dependent manner (Fig. 3E) in the presence of an AMPA receptor inhibitor (GYKI 52466). Second, consistent with the results found by Mott et al. (2008), incubation of cortical cultures with 100 μM CNQX significantly reduced the KAR-mediated AMPA-induced calcium transient, whereas a lower, AMPA receptor–specific concentration (1.5 μM) in the presence of GYKI 52466 did not (Fig. 3F). Third, SYM2081 (a potent KAR agonist) as low as 1 nM could elicit substantial Ca^{2+} signals (Fig. 3, G and H) similar to that found for homomeric and heteromeric KARs expressed in HEK cells (Alt et al., 2004). Micromolar concentrations of SYM2081 were needed to activate AMPA receptors (Donevan et al., 1998). Fourth, voltage-dependent Ca^{2+} channels (VDCC) do not contribute to the observed increase in the calcium transient after activation of group I mGlu receptors and PKC. KCl (12 mM) was added to the cortical cultures in the presence of NMDA, AMPA, kainate, and $GABA_A$ receptor blockers (10 μM MK801 plus 100 μM D-AP5, 100 μM GYKI 52466, 500 μM CNQX, 500 μM NBQX, and 100 μM bicuculline), resulting in an increase in cytosolic Ca^{2+} (Fig. 3D) attributed to depolarization-mediated activation of VDCCs. After group I mGlu activation by DHPG (50 μM) application or PKC activation by PMA (100 nM), the VDCC-dependent Ca^{2+} transient was slightly inhibited in cortical cultures rather than potentiated (Fig. 3D), suggesting that VDCC opening does not contribute to the potentiation of KARs by group I mGlu activation. Taken together, these data suggest that native kainate receptors but not AMPA receptors in cortical cultures lead to the calcium transients in the presence of NMDA, AMPA, and $GABA_A$ receptor blockers and are potentiated by activation of group I mGlu receptors. Protein kinase C is likely to be involved in this modulation.

Activation of Group I but not Group III mGlu Receptors Potentiates Recombinant Heteromeric KARs. The KAR subunit composition sensitive to mGlu signaling remains unknown. To address this issue, we coexpressed specific KARs along with various mGlu receptors in *X. laevis* oocytes. In oocytes coexpressing KARs with mGlu1, typical inward currents were elicited by 30 μM AMPA for heteromeric KARs (assemblies of GluK2 and either GluK4

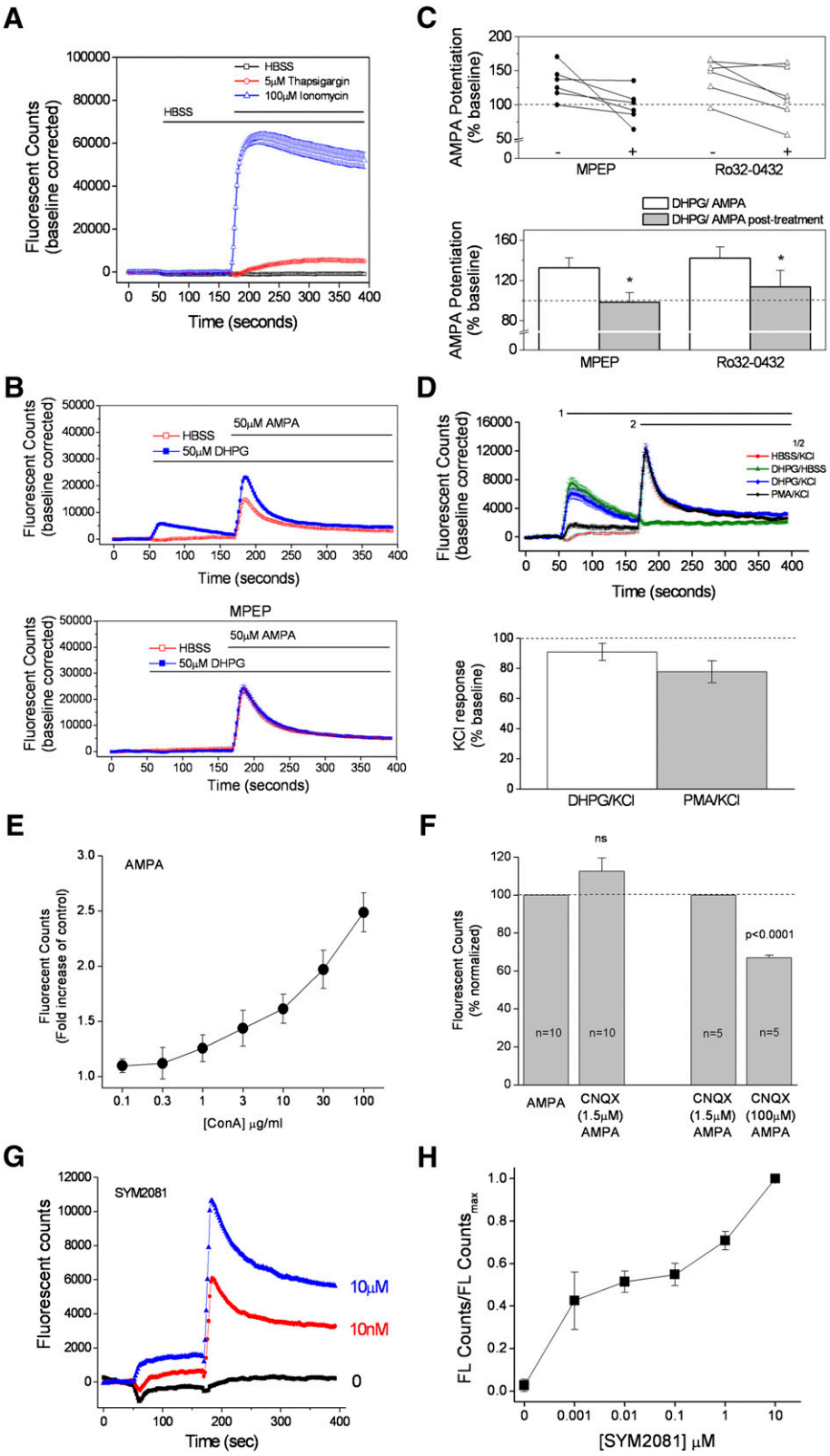

Fig. 3. Activation of group I mGlu receptors potentiates KARs in rat cortical cultures. (A) Ca^{2+}-dependent fluorescent signal of cortical cultures loaded with Fluo-4 was monitored. With use of the integrated fluidics of the FLEXStation, a bolus of HBSS was delivered at 60 seconds, resulting in a miniscule reduction in the fluorescent signal. At 180 seconds, addition of ionomycin (100 μM) or thapsigargin (5 μM) resulted in a long-lasting increase in the $[Ca^{2+}]_i$. Data are the mean of eight replicates from a single plate. (B) in cultures pretreated with NMDA, AMPA, and $GABA_A$ receptor blockers (10 μM MK801, 100 μM D-AP5, 100 μM GYKI 52466, and 100 μM bicuculline), a similar rapid increase in fluorescence was detected after application of DHPG (50 μM) and AMPA (50 μM). The DHPG-induced potentiation of the AMPA response was blocked by preincubation with 4 μM MPEP. Data are the mean of eight replicates from a single plate. Bars indicate the duration of drug exposures. (C) MPEP (4 μM, $n = 6$) and Ro 320432 (4 μM, $n = 6$) prevented DHPG-induced KAR potentiation. Data are the mean and standard error of paired t tests ($^*P < 0.05$). (D) in cultures pretreated with NMDA, AMPA, kainite, and $GABA_A$ receptor blockers (10 μM MK801, 100 μM D-AP5, 500 μM CNQX, 500 μM NBQX, 100 μM GYKI 52466, and 100 μM bicuculline), a rapid increase in fluorescence was detected after application of KCl (12 mM) and DHPG (50 μM). Activation of group I mGlu receptors by DHPG slightly reduced the KCl-induced calcium transient. Data are the mean of eight replicates from a single plate. Bars indicate the duration of drug exposures. The panel below shows that the calcium transients elicited by KCl were not potentiated by DHPG or PMA ($n = 12$ experiments from two independent culture preparations). (E) in cultures pretreated with NMDA, AMPA, and $GABA_A$ receptor blockers (10 μM MK801, 100 μM D-AP5, 100 μM GYKI 52466, and 100 μM bicuculline), a similar rapid increase in fluorescence was detected after application of AMPA (50 μM). AMPA-induced increase in intracellular calcium was increased by exposure to the KAR potentiator ConA in a dose-dependent manner. Data are the mean S.E. of four experiments from a single culture. (F) In cultures pretreated with NMDA, AMPA, and $GABA_A$ receptor blockers, the AMPA-induced increase in fluorescent counts was significantly blocked by a high (100 μM) but not a low (1.5 μM) concentration of CNQX. (G) in cultures pretreated with NMDA, AMPA, and $GABA_A$ receptor blockers, a similar rapid increase in fluorescence was detected after application of the KAR agonist SYM2081. (H) the SYM2081-induced increase in intracellular calcium was dose-dependent. Data are the mean of the peak calcium signal and standard error of three experiments from two independent cultures.

or GluK5 subunits) and by 10 μM domoic acid for homomeric GluK1 and GluK2 KARs (Fig. 4A). Agonist responses were absent in uninjected oocytes or oocytes injected with vehicle only (no mRNA). After baseline responses to repeated agonist exposure had stabilized, the mGlu agonist ACPD (100 μM) was applied for 2 minutes. After mGlu1 activation, the GluK2/GluK4 and GluK2/GluK5 receptors showed significant potentiation, compared with the baseline: 138 $\pm$ 7.8% ($n = 5$) and 197 $\pm$ 19.3% ($n = 16$), respectively (Fig. 4, A and C). Activation of mGlu1 had little to no effect on homomeric GluK1 and

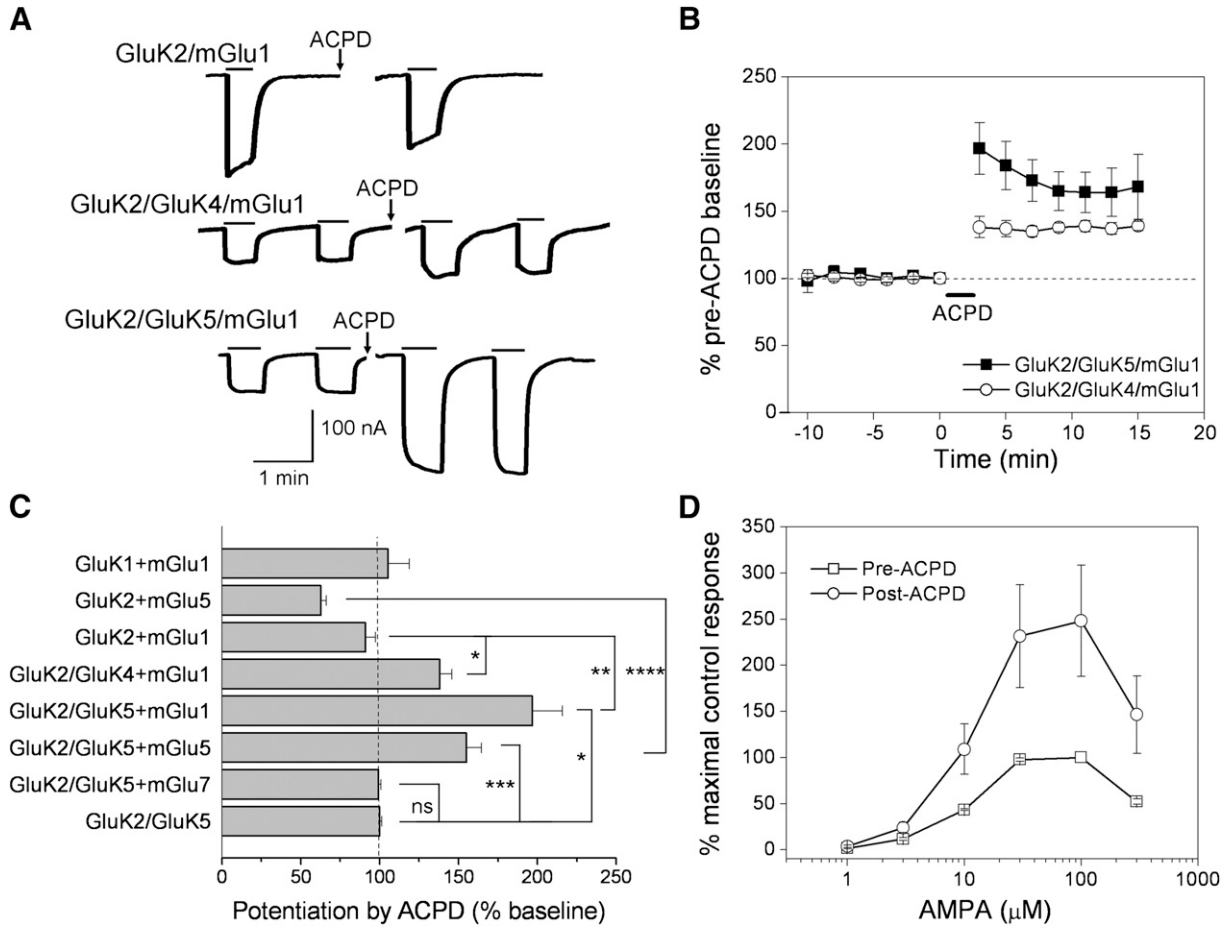

Fig. 4. Potentiation of heteromeric KARs by group I mGlu activation. (A) whole-cell currents were recorded from oocytes 3 days after injection with mRNAs encoding GluK2/mGlu1, GluK2/GluK4/mGlu1, or GluK2/GluK5/mGlu1. After application of 100 μM ACPD (a nonspecific mGlu activator), steady-state activation of the heteromeric receptors by AMPA (30 μM) was potentiated, but not steady-state activation of the homomeric KAR by domoic acid (10 μM). (B) time-dependent potentiation of GluK2/GluK4/mGlu1 and GluK2/GluK5/mGlu1 AMPA currents by mGlu1 activation with ACPD (n = 5 and n = 16, respectively). (C) varying the subunit combination of the KAR and mGlu receptors revealed significant ACPD potentiation of only the heteromeric KARs expressed together with group I mGlu receptors ($n \geq 4$). The largest ACPD-mediated potentiation was seen in oocytes expressing GluK2/GluK5/mGlu1 (n = 16) (*$P < 0.05$, **$P < 0.01$, ***$P < 0.005$, ****$P < 0.0001$, ns=not significant; one-way ANOVA with selected Bonferroni's post-tests). (D) AMPA concentration-response curves from oocytes expressing GluK2/GluK5/mGlu1 before and after mGlu activation revealed potentiation at multiple AMPA concentrations with no apparent difference in the concentration ranges over which kainate receptors are activated and desensitized (n = 4).

GluK2 responses (Fig. 4, A and C). However, activation of mGlu5 inhibited homomeric GluK2 perhaps via rundown of the current after activation of mGlu5 or via an intrinsic difference in the two GPCRs (see *Discussion*). Nevertheless, significant potentiation was only observed after activation of the group I mGlu receptors expressed with heteromeric KARs. The mGlu1-mediated potentiation of heteromeric GluK2/GluK4 and GluK2/GluK5 currents was maximal within the first two minutes after exposure to ACPD and persisted for at least 15 minutes (Fig. 4B). We have recorded potentiation lasting up to 25 minutes. However, the stability of the oocyte recording complicates the data from longer recordings. Thereafter, all experiments involving mGlu activation were performed with a minimum exposure of 2 minutes.

The mGlu1 and mGlu5 receptors are GPCRs coupled to $G\alpha_q$. To determine whether mGlu receptors that couple to a different G-protein also modulate KARs, similar experiments were performed on oocytes coexpressing heteromeric KARs with mGlu7 (a member of the group III subfamily). In oocytes coexpressing GluK2/GluK5 and mGlu7, activation of mGlu7 with 100 μM ACPD, 500 μM L-AP4 [L-(+)-2-amino-4-phosphonobutyric acid], or 10 μM AMN082 [*N,N′*-bis(diphenylmethyl)-1,2-ethanediamine] did not affect AMPA-mediated KAR currents (99 ± 1.61% of control [n = 4 Fig. 4C]; 107 ± 2.94% of control [n = 4]; 107 ± 4.49% of control [n = 8], respectively). This suggests that the $G_{\beta\gamma}$ subunit of the G-protein may not influence GluK2/GluK5, in contrast to its effects on the G protein–coupled inwardly rectifying potassium channels (Dascal, 1997). Potentiation of GluK2/GluK5 after bath application of ACPD was observed only in oocytes coexpressing mGlu1 or mGlu5 (Fig. 4C)

Recently, it has been demonstrated that heteromeric KARs containing GluK4 or GluK5 subunits exhibit bell-shaped biphasic steady-state concentration-response curves in response to glutamate or AMPA, whereas homomeric GluK2 exhibits a monophasic steady-state concentration-response curve to glutamate and is insensitive to AMPA (Mott et al., 2010). The bell-shaped steady-state concentration-response curves to AMPA and glutamate observed in the heteromeric KARs are attributed to high and low agonist affinity sites in

heteromeric KARs, causing activation and desensitization, respectively (Mott et al., 2010). To determine whether activation of mGlu1 alters the potency with which AMPA activates heteromeric KARs, the AMPA concentration-response relationships with or without preceding activation of mGlu1 were compared. Activation of mGlu1 by ACPD increased the KAR current across a range of AMPA concentrations, but did not alter AMPA potency (Fig. 4D). Moreover, the downward limb of the AMPA concentration-response curve was as prominent after potentiation as previously, suggesting that potentiation by group I mGlu receptors is not caused by relief from desensitization (Mott et al., 2010).

Activation of mGlu1 and mGlu5 by the group I specific receptor agonist DHPG significantly potentiated GluK2/GluK5 currents in a similar manner as ACPD (162 ± 10.8% of control [$n = 10$] for mGlu1 and 138 ± 4.9% of control [$n = 6$] for mGlu5) (Fig. 5). CHPG, a selective mGlu5 agonist, also potentiated GluK2/GluK5 when coexpressed with mGlu5 ($n = 4$). DHPG failed to potentiate GluK2/GluK5 in the absence of mGlu1 or mGlu5. Similarly, no potentiation was observed in oocytes coexpressing GluK2/GluK5 and mGlu1 after exposure to 100 μM DCG IV (a group II mGlu agonist) (Fig. 5). Taken together, these results indicate that heteromeric KARs containing GluK2 in combination with GluK4 or GluK5 subunits are modulated by group I mGlu receptors, with heteromers containing GluK5 showing the highest potentiation.

Although both mGlu1 and mGlu5 activation potentiated heteromeric KARs, the degree of potentiation was larger for mGlu1 than for mGlu5, either in oocytes or cultured cortical neurons. We therefore decided to take advantage of this robust potentiation and focus on mGlu1 to investigate the importance of key signaling molecules in the intracellular signaling cascade after mGlu1 activation. Hereafter, experiments were performed to determine the molecular basis for the modulation of GluK2/GluK5 by mGlu1 activation.

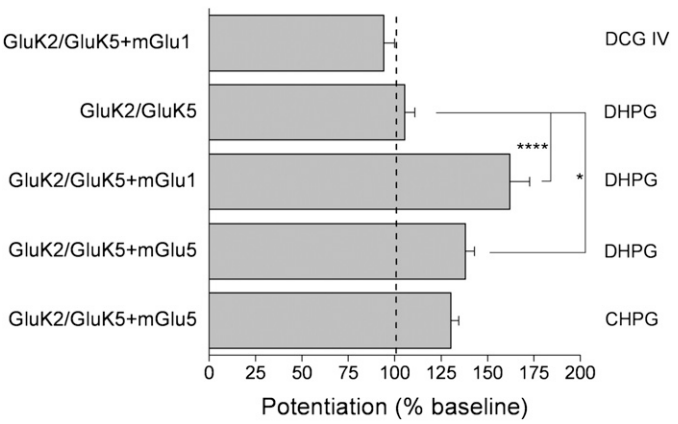

Fig. 5. Selective modulation of GluK2/GluK5 by group I mGlu activation. Whole-cell currents were recorded from oocytes 3 days after injection with GluK2/GluK5, GluK2/GluK5/mGlu1, and GluK2/GluK5/mGlu5 mRNAs. AMPA steady-state currents from GluK2/GluK5/mGlu1 and GluK2/GluK5/mGlu5 were significantly potentiated after application of DHPG ($n \geq 4$, $^*P < 0.05$, $^{****}P < 0.001$; one-way ANOVA with Bonferroni's post-tests). DHPG had a minuscule effect on GluK2/GluK5 in the absence of either group I mGlu receptor ($n = 6$). CHPG (a selective mGlu5 agonist) produced a similar potentiation of GluK2/GluK5/mGlu5 as DHPG ($n = 4$). Bath application of the group II mGlu agonist DCG IV had no effect.

mGlu1 Mediated Potentiation Requires PLC Activation and Ca^{2+} Mobilization. mGlu1 and mGlu5 share a common intracellular second messenger cascade after ligand binding that involves activation of molecules, such as $G\alpha_q$, phospholipase C, and protein kinase C (PKC). Therefore, we determined whether such key players in this intracellular second messenger cascade were necessary for the potentiation of GluK2/GluK5 receptors by mGlu1 and mGlu5. GDPβS (a nonhydrolyzable GDP analog that interferes with the binding of GDP) was used to determine whether active G-protein signaling was necessary for mGlu1-mediated potentiation. Oocytes coexpressing GluK2/GluK5 and mGlu1 were injected immediately prior to recording with 50 nl of either GDPβS (10 mM) or vehicle. GDPβS nearly eliminated the mGlu1-mediated potentiation, 120 ± 11.1% of control ($n = 5$) for GDPβS treatment versus 209 ± 26.5% of control ($n = 12$) for vehicle (Fig. 6A), suggesting that G-protein signaling rather than a β-arrestin-like pathway is necessary for KAR potentiation. Furthermore, the phospholipase C (PLC) inhibitor U73122 (10 μM) abolished mGlu1-mediated GluK2/GluK5 potentiation, compared with oocytes exposed to its inactive isomer U73343 (10 μM) (Fig. 6A).

A downstream consequence of activation of group I mGlu receptors is an increase in intracellular Ca^{2+} as described above in our calcium assay experiments. During the recordings in oocytes, large calcium-activated Cl^- currents were observed after activation of the mGlu1 or mGlu5 receptors. To determine whether an increase in intracellular Ca^{2+} is required for the mGlu1 mediated potentiation of GluK2/GluK5, oocytes coexpressing GluK2/GluK5 and mGlu1 were injected with 100 nl of the Ca^{2+} chelator BAPTA (100 mM) prior to recording. BAPTA eliminated the potentiation of KAR responses by mGlu1 (100 ± 6.39% of control [$n = 7$]) (Fig. 6A). Together, these results suggest that, after activation of mGlu1, a signaling pathway involving the G_α-protein, PLC, and an increase in intracellular Ca^{2+} are necessary for potentiation of the GluK2/GluK5 receptor.

Involvement of PKC in the Potentiation of KARs by mGlu1 Activation. PLC activation together with an increase in intracellular Ca^{2+} is required for the activation of PKC. To determine whether PKC is involved in the potentiation of GluK2/GluK5 receptors by mGlu1 activation, the effects of the general protein kinase inhibitor staurosporine and the selective PKC inhibitor Ro 320432 were explored. Preincubation of oocytes with staurosporine (100 nM) caused a substantial attenuation of the mGlu1mediated effect to 113 ± 4.48% of control ($n = 6$) (Fig. 6, A and B). The time profile shows that the effect of staurosporine lasted throughout the entire recording (Fig. 6B). Pretreatment with Ro 320432 (2 μM) also showed a similar attenuation of the ACPD-mediated KAR potentiation (Fig. 6A). We conclude that PKC activation is a necessary step for potentiation; it is also sufficient (see below).

Potentiation of NMDA receptors occurs via mechanisms involving PKC or Src tyrosine kinases (Kelso et al., 1992, Wang and Salter, 1994, Chen and Leonard, 1996, Kohr and Seeburg, 1996). Therefore, experiments were performed to determine whether Src tyrosine kinases might also be involved in the potentiation of GluK2/GluK5. Preincubation with genistein (50 μM), a broad-spectrum but nonspecific tyrosine kinase inhibitor, also reduced the KAR potentiation after mGlu1 activation (Fig. 6A). Of note, at 50 μM, genistein

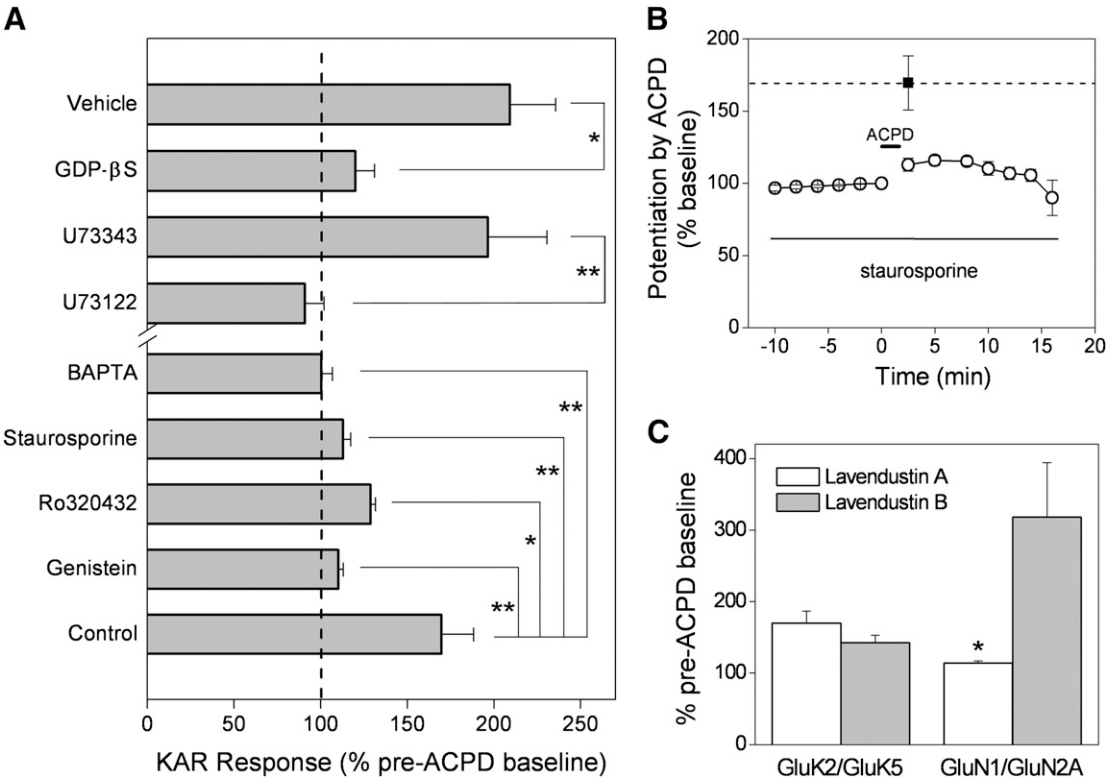

Fig. 6. Dependence on G-protein, PLC, Ca^{2+}, and PKC. (A) whole-cell currents were recorded from oocytes 3 days after injection of GluK2/GluK5/mGlu1 mRNAs. Before recording, injection of oocytes with 50 nl of GDPβS (10 mM) strongly reduced the ACPD-induced potentiation, compared with vehicle-injected cells ($n = 5$ and $n = 12$, respectively) ($^*P < 0.05$; t test). The PLC inhibitor U73122 (10 μM) abolished ACPD-induced potentiation, but the inactive isomer U73343 (10 μM) did not ($n = 10$ and $n = 8$, respectively) ($^{**}P < 0.01$; t test). Injection of BAPTA (100 mM, 100 nl) also blocked ACPD-induced potentiation of GluK2/GluK5/mGlu1 ($n = 7$). The broad spectrum kinase inhibitor staurosporine (100 nM), genistein (50 μM), and the specific PKC inhibitor Ro 320432 (2 μM) dramatically reduced ACPD-mediated potentiation in oocytes injected with GluK2/GluK5/mGlu1 ($n \geq 4$ $^*P < 0.05$, $^{**}P < 0.01$; one-way ANOVA with Dunnett's post-test, each compared with control). (B) the time-dependent potentiation of GluK2/GluK5/mGlu1 currents by ACPD was reduced by staurosporine ($n \geq 4$). Note that exposure to staurosporine blocked the ACPD mediated potentiation during the entire recording. The filled square and dashed line indicates the normal peak level of potentiation ($\pm$ S.E.M.) in the absence of staurosporine ($n = 6$). (C) pretreatment of oocytes with the specific src-tyrosine kinase inhibitor lavendustin A blocked ACPD-mediated potentiation of NMDA receptors (GluN1/GluN2A/mGlu1) ($n = 3$, $^*P < 0.05$; t test) but failed to significantly inhibit the potentiation of GluK2/GluK5/mGlu1 ($n = 9$).

also inhibits PKC (Akiyama et al., 1987, Geissler et al., 1990). Exposure of oocytes to lavendustin A, a potent and specific inhibitor of Src tyrosine kinase, dramatically reduced the mGlu1-mediated potentiation of NMDA receptors but had no effect on heteromeric GluK2/GluK5 (Fig. 6C). Lavendustin B, the inactive analog incapable of inhibiting Src tyrosine kinases, had no effect on either receptor (Fig. 6C). These data suggest that the mGlu1 regulation of the GluK2/GluK5 receptor is mediated by PKC but not by Src- or tyrosine kinase activation, in contrast to mGlu1-mediated potentiation of NMDA receptors, which involves Src.

Direct Activation of PKC Potentiates Heteromeric KARs. Oocytes expressing heteromeric GluK2/GluK5 were exposed to PMA, an analog of diacylglycerol that stimulates PKC. PMA (50 nM), but not its vehicle (DMSO) or the inactive 4α PMA analog, caused a strong potentiation of the heteromeric GluK2/GluK5 (170 $\pm$ 9% of control [$n = 12$]) (Fig. 7A–C). Thymeleatoxin (1 μM), which selectively activates the conventional PKC isoforms (α, β, γ), also potentiated GluK2/GluK5 receptors (143 $\pm$ 19.2% of control; $n = 8$), suggesting that at least one of the conventional PKC isoforms is involved (Fig. 7C). The specific PKC inhibitor Ro 320432 attenuated the effect of PMA (Fig. 7, B and E). The general tyrosine kinase inhibitor genistein also reduced the effect of PMA on GluK2/GluK5 (Fig. 7E), again perhaps via nonspecific inhibition by genistein. Of interest, PMA potentiated GluK2/GluK4 to a similar degree as GluK2/GluK5 but failed to significantly potentiate homomeric GluK2 (109 $\pm$ 5.2% of control; $n = 10$) (Fig. 7E). If direct activation of PKC results in potentiation of GluK2/Gluk5 via phosphorylation, then inhibition of phosphatases may further enhance the effect of PKC. To test this possibility, oocytes were incubated before and during recording in 20 nM okadaic acid, a cell permeable inhibitor of PP1 and PP2A phosphatases. After incubation in okadaic acid, the potentiation was large and did not fade for the duration of the recording (Fig. 7D), suggesting that the fade observed is attributable to activation of protein phosphatases.

The direct activation of PKC affected GluK2/GluK5 receptors to the same degree as activation of mGlu1, reinforcing a mechanism regulating KARs involving PKC. Strengthening this idea is the finding that the GluK2/GluK5 potentiation by PMA (averaging 50–70% in different batches of oocytes) was significantly attenuated to 21% in 5 oocytes that had been prepotentiated by mGlu1 activation (Fig. 8). A similar finding was obtained by reversing the order of exposure of PMA and ACPD. Prepotentiation of GluK2/GluK5 by PMA occludes mGlu1 dependent enhancement (data not shown). These data suggest that convergent pathways are engaged.

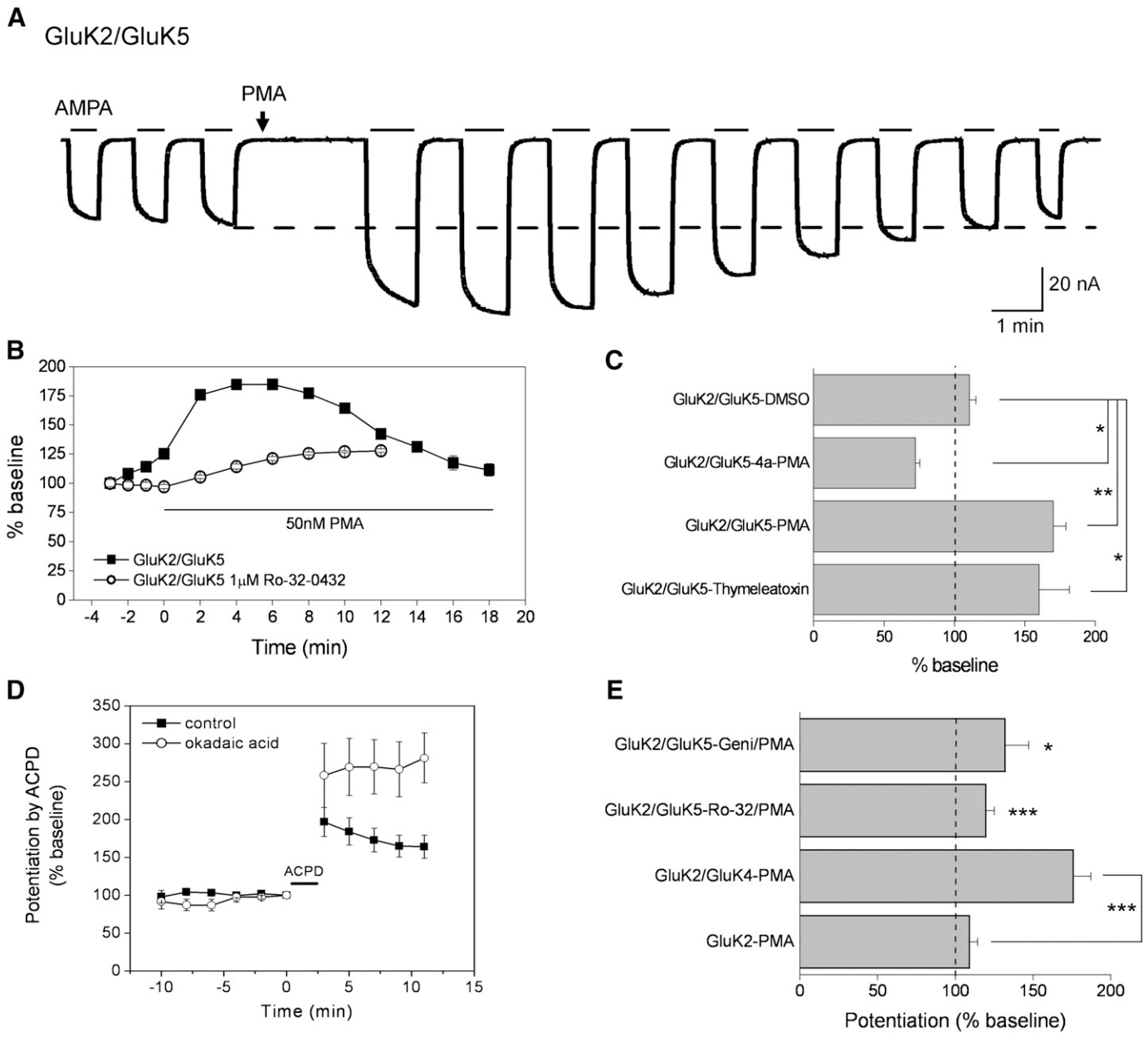

Fig. 7. PKC activation potentiates heteromeric KARs. (A) AMPA steady-state currents were recorded from an oocyte three days after injection of GluK2/GluK5. Bath application of the phorbol ester PMA (50 nM) led to a biphasic response on AMPA elicited currents. (B) the time profile showed a fast potentiation followed by slow decrease in the currents. The specific PKC inhibitor Ro 320432 (2 μM) dramatically reduced PMA-mediated potentiation in oocytes injected with GluK2/GluK5 ($n \geq 8$). (C) activation of PKC by PMA potentiated heteromeric GluK2/GluK5 ($n = 12$). Neither DMSO alone nor 4α-PMA (an inactive analog of PMA) mimicked the PMA induced potentiation of GluK2/GluK5 ($n = 6$ and $n = 5$, respectively). GluK2/GluK5 AMPA steady-state currents were also potentiated by exposure to 1 μM thymeleatoxin (an activator of the conventional PKC isoforms α, β, γ) ($n = 6$) (*$P < 0.05$; **$P < 0.01$; one-way ANOVA with Dunnett's post-tests). (D) okadaic acid (20 nM) treatment enhanced PMA-induced potentiation of GluK2/GluK5 ($n = 5$). The filled squares indicate the normal level of potentiation (± S.E.M.) in the absence of okadaic acid. (E) genistein (Geni) (50 μM) pretreatment reduced the PMA induced potentiation of GluK2/GluK5 ($n = 5$). The specific PKC inhibitor Ro 320432 (2 μM) strongly attenuated the effect of 50 nM PMA. The effects of genistein and Ro 320432 were compared with GluK2/GluK5 exposed to PMA (C) and were found to be significantly different. Activation of PKC by PMA also potentiated heteromeric GluK2/GluK4 receptors, but failed to significantly potentiate homomeric GluK2 (*$P < 0.05$; **$P < 0.01$; ***$P < 0.05$; one-way ANOVA with Bonferroni's post-tests).

The C Terminus of GluK5 Is Critical for the Potentiation of GluK2/GluK5 Receptors. The results described above suggest that a serine/threonine phosphorylation event underlies potentiation of the GluK2/GluK5 receptor by mGlu1. The long C terminus of GluK2 is phosphorylated by PKA on serine residues 825 and 837, which potentiates homomeric receptor activation in whole cell patch studies (Kornreich et al., 2007), apparently through an increase in receptor open probability (Traynelis and Wahl, 1997). Phosphorylation of serines 879 and 885 of GluK1 by PKC results in internalization of the subunit (Rivera et al., 2007). However, phosphorylation sites on GluK4 or GluK5 have not yet been identified (Traynelis et al., 2010). Because PKC-mediated potentiation of heteromeric KARs by mGlu1 is stronger for receptors with GluK5 than for those with GluK4 (Fig. 4C), we examined the role of the intracellular domains of

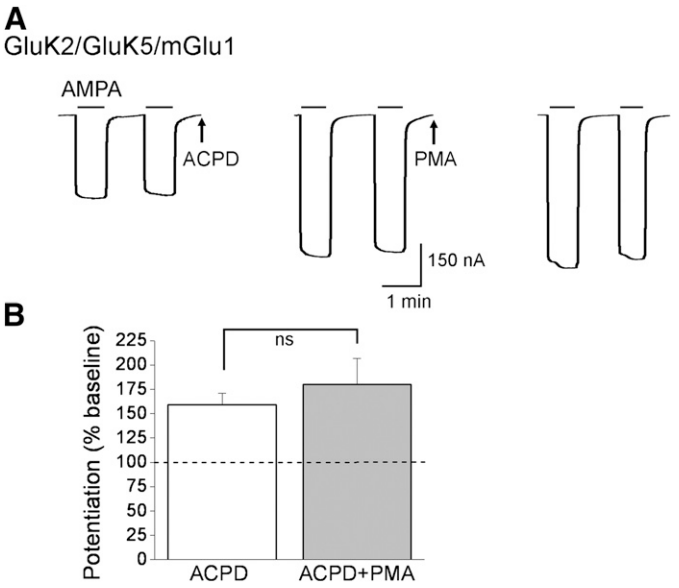

Fig. 8. Potentiation by ACPD and PMA is nonadditive. (A) AMPA steady-state currents were recorded from an oocyte expressing GluK2/GluK5/mGlu1. After exposure to 100 μM ACPD, the cell was subsequently treated with 50 nM PMA. Prior exposure to ACPD resulted in a much lower response to PMA. (B) quantification under the same conditions as in A demonstrates that the potentiation of ACPD and PMA is not additive ($n \geq 4$).

GluK5 in the potentiation. The predicted C-terminal intracellular domain of GluK5 is large, with over 160 amino acid residues and numerous serine and threonine residues, many of which are consensus PKC phosphorylation sites (Fig. 9A). To identify critical regions of the C-terminal domain required for mGlu1-mediated potentiation of GluK2/GluK5 receptors, we first constructed two truncation mutants by insertion of a stop codon immediately after serine 836 (GluK5Δ837) or methionine 883 (GluK5Δ884) (Fig. 9A). The two truncation mutants were coexpressed with GluK2 and mGlu1 in *X. laevis* oocytes. Agonist responses for both mutants were typical for KARs; the truncated GluK5 constructs did not affect the size of the currents nor agonist sensitivity. The GluK5Δ884 mutant responded similarly as full-length GluK5 after mGlu1 activation; however, potentiation was abolished in GluK5Δ837 (Fig. 9B), suggesting that a specific region near or between positions 836 and 883 was critical for mGlu1-mediated potentiation of heteromeric GluK2/GluK5.

Identification of Potential Phosphorylation Sites. A scan of the C terminus of GluK5 revealed several potential PKC phosphorylation sites within the C-terminal domain. There are seven strong PKC consensus sites [i.e., R(K)–X_{0-2}–T/S–X_{0-2}–R(K)] in the region between positions 836 and 883 in GluK5 and an additional two located just upstream of position 836 (red residues in Fig. 9A). These predicted sites were replaced individually by an alanine residue or in double, triple, or quadruple combinations. The potentiation of each mutant was normalized to that of the wild-type GluK2/GluK5 receptor recorded in the same batch of oocytes on the same day. To our initial surprise, double mutations of serine/threonine residues within the 836–884 region had no significant effect on mGlu1-mediated potentiation (Fig. 9C). This was unexpected, considering the results of the two truncation mutants. However, mutating three serines together around the 837 truncation site to alanines (GluK2/GluK5-S833A/S836A/S840A) virtually abolished the mGlu1-mediated KAR potentiation (Fig. 9, C and D), suggesting that these residues are crucial for GluK2/GluK5 potentiation after mGlu1 activation.

To explore whether these three serines might be phosphorylation sites, we first converted all three residues to aspartate to produce constitutively negatively charged residues that might mimic phosphorylation of the receptor. The GluK5 triple mutant (GluK5-S833D/S836D/S840D) was coinjected with GluK2 in *X. laevis* oocytes. KAR currents in the heteromeric KAR carrying the triple D mutations were more than doubled in amplitude when compared with the wild-type counterpart recorded on the same day (372 ± 51 nA [$n = 20$] for GluK2/GluK5-S833D/S836D/S840D versus 163 ± 30 nA [$n = 18$] for wild-type; $P < 0.01$) (Fig. 10, A and C). Subsequently, the effect of the PMA-induced potentiation on this mutant was tested. The triple aspartate mutant was not further potentiated by exposure to PMA (110 ± 6% of control; $n = 14$), whereas the wild-type recorded at the same time was (152 ± 10% of control; $n = 13$; $P < 0.01$) (Fig. 10, A and B).

We then converted the same three serines to glutamate (GluK5-S833E/S836E/S840E) and found that potentiation is retained (Fig. 10B) and basal currents are of normal amplitude (Fig. 10C), contrary to the results with the triple-D mutant but consistent with the notion that residues in addition to Ser833/Ser836/Ser840 might be PKC targets. To explore a potential contribution by other serine and threonine residues to the GluK5-TE phenotype, we first created a mutant GluK5 receptor that included seven substitutions (i.e., GluK5-S833E-S836E-S840E-S854A-T858A-S859A-S861A), all of which are predicted by phosphorylation prediction software to be potential PKC phosphorylation sites. Unfortunately, when combined with GluK2, this mutant receptor containing seven substitutions in this very critical domain failed to produce functional currents. A similar mutant receptor with aspartate substitutions at the four downstream sites (GluK5-S833E-S836E-S840E-S854D-T858D-S859D-S861D) also failed to produce functional currents. Two clones of each construct were tested using two separate batches of oocytes. We then created a GluK5 mutant bearing a truncation at position 884, together with the S833E, S836E, and S840E mutants (i.e., GluK5-TE-Δ884). This mutant produced functional agonist-induced currents in oocytes when combined with GluK2 and mGlu1. However, in contrast to the GluK5-TE (Fig. 10B) and GluK5-Δ884 (Fig. 9B), which both show normal potentiation after mGlu1 or PMA activation, the combination GluK2/GluK5-TE-Δ884 construct showed no potentiation either by mGlu1 (81 ± 9% of control; $n = 8$) or PMA (107 ± 8% of control; $n = 14$) (Fig. 10, D and E). Together, these results suggest that the three proximal serine residues (Ser833, Ser836, Ser840) act in concert with downstream residues in PKC-mediated potentiation of heteromeric KARs.

Discussion

In this study, we show for the first time the functional contribution of the high-affinity KAR subunits to modulation by group I metabotropic glutamate receptors. GluK4 and GluK5 heteromeric combinations with GluK2 bestow modulation by both group I metabotropic glutamate receptors and

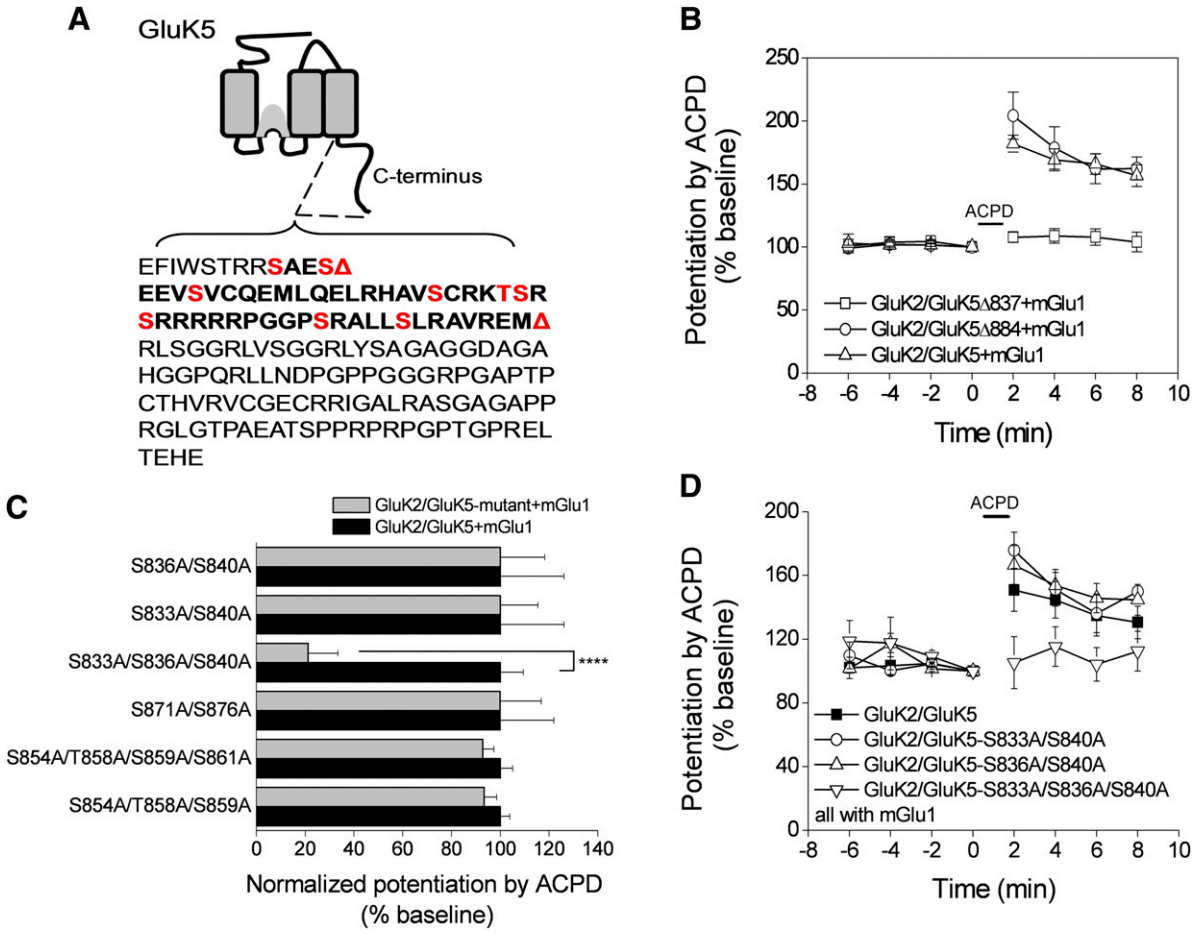

Fig. 9. Identification of a critical domain. (A) schematic showing the GluK5 C-terminal domain. The first red triangle indicates the location of an inserted stop codon (Δ837) and the second red triangle indicates the position of a more distal stop codon (Δ884). The red residues indicate consensus PKC phosphorylation sites. (B) truncation of the GluK5 C terminus at 837, but not 884, blocked ACPD-induced potentiation of GluK2/GluK5 when coexpressed with mGlu1 ($n \geq 4$). (C) alanine mutagenesis of the C-terminal serines and threonines between 833 and 883 revealed that only the triple GluK5 mutant (GluK5-S833A/S836A/S840A) resulted in a significantly reduced ACPD mediated potentiation when combined with GluK2 and mGlu1 ($n \geq 4$, $^{****}P < 0.001$; t test). (D) the time-dependent potentiation of GluK2/GluK5/mGlu1 by ACPD was not seen in the GluK5 triple alanine mutant (GluK5-S833A/S836A/S840A) ($n \geq 4$).

PKC onto the resulting heteromeric receptors. Our results point to the potentiation of heteromeric kainate receptors by class I mGlu receptor activation being mediated by phosphorylation of GluK5 by PKC in the proximal C terminus. These findings predict a modulatory role of the high-affinity KAR subunits in synaptic transmission and plasticity.

Subunit selective antibodies raised to GluK4, GluK5, mGlu1, and mGlu5 revealed the distribution of these proteins in the rat hippocampus. The pattern of KAR expression in the hippocampus observed in this study is consistent with earlier reports (Bureau et al., 1999, Darstein et al., 2003, Ruiz et al., 2005). For the first time, however, we present evidence for subcellular colocalization of the high-affinity protein KAR subunits with group I metabotropic glutamate receptor subunits in the hippocampus. Our results indicate that the high-affinity KAR subunits and group I metabotropic glutamate receptors are colocalized within the volume of individual pixels (0.62 μm^3) in the dendrite-rich strata lucidum and radiatum of the CA3 region of the hippocampus, which satisfies a critical requirement for functional cross-talk in synaptic transmission and plasticity, namely that the proteins should be located in close proximity.

The finding that DHPG potentiates KAR-induced Ca^{2+} signals in rat cortical culture in a PKC-dependent manner (Fig. 3) is consistent with results reported by Cho et al. (2003) and demonstrates that group I metabotropic glutamate receptor activation potentiates KAR-mediated calcium signaling. However, their potentiation appeared to be independent of an increase in intracellular calcium, in contrast to our findings (Fig. 6A). These contrasting observations point to multiple pathways by which potentiation can proceed. Of interest, Selak et al. (2009) reported reduced GluK5-dependent KAR activity after group I mGlu activation, which was attributed to endocytosis of GluK5 via PKC-mediated disruption of the interaction of GluK5 with the synapse interacting proteins SNAP-25 and PICK1. The authors suggested that PKC interacts with PICK1, resulting in disruption of the SNAP-25-PICK1-GluK5 complex. Additional studies also suggest regulation of surface expression of GluK2 by its PKC phosphorylation, although by analogy to our study, the phosphorylation site identification is inconclusive, because mutagenesis of the putative serines to all three relevant residues (Ala, Asp, and Glu) was not done (Nasu-Nishimura et al., 2010, Konopacki et al., 2011, Chamberlain et al., 2012).

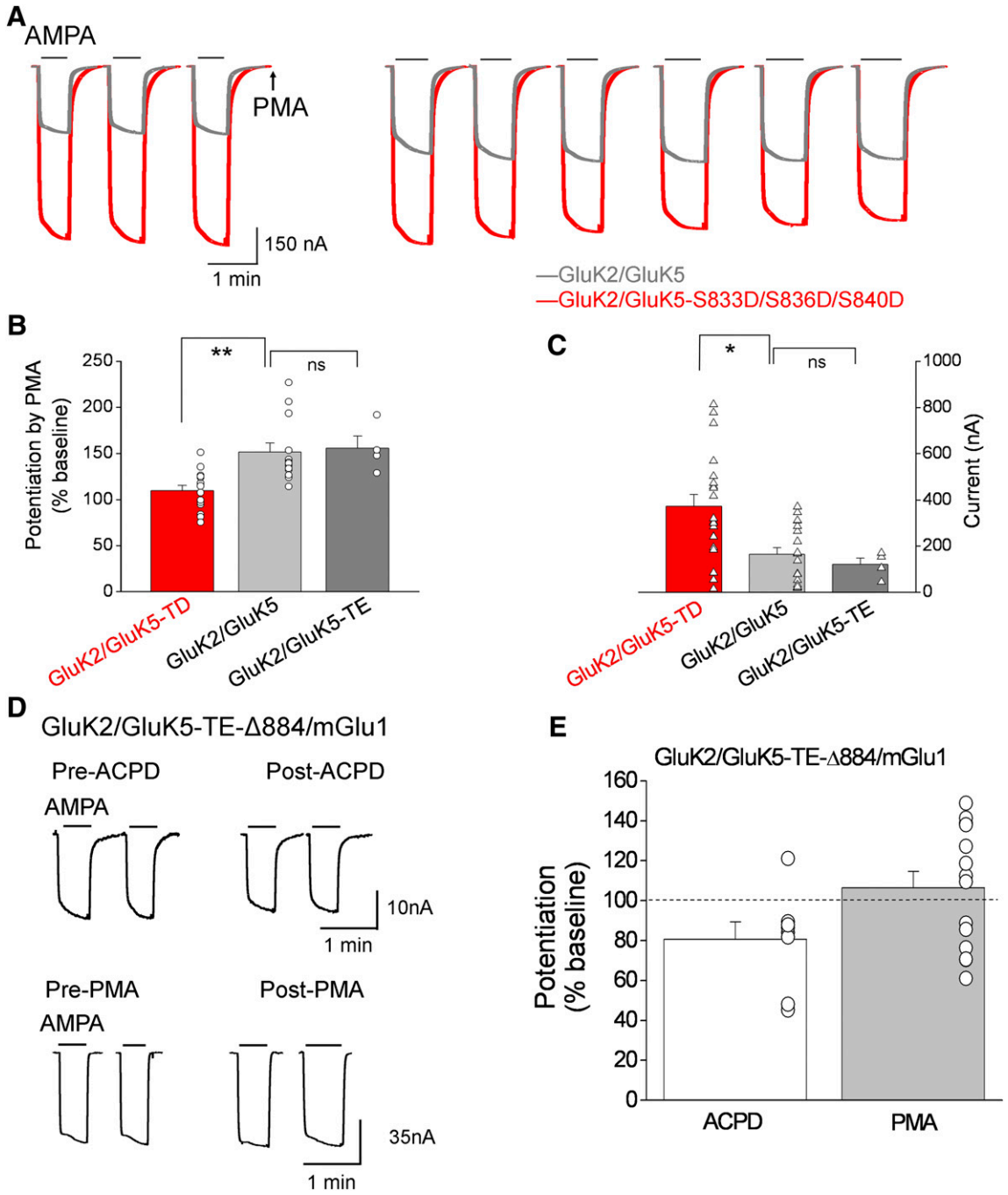

Fig. 10. PKC phosphorylation sites. (A) mutation of three serines (Ser833, Ser836, and Ser840) in GluK5 to aspartate nearly eliminated potentiation by PMA, compared with wild-type. (B) this pseudo-phosphorylated mutant GluK2/GluK5-S833D/S836D/S840D (GluK2/GluK5-TD) but not the triple glutamate (TE) mutant showed reduced potentiation by PMA ($n \geq 4$, $^{**}P < 0.01$; one-way ANOVA with Bonferroni's post-test). The triple-D mutant also demonstrated larger whole-cell currents (C), compared with GluK2/GluK5-S833E/S836E/S840E (GluK2/GluK5-TE) or the wild-type ($n \geq 4$, $^{**}P < 0.01$; one-way ANOVA with Bonferroni's post-test). (D) the GluK5-S833E-S836E-S840E-Δ884 mutant coexpressed with GluK2 and mGlu1 displayed normal currents, no potentiation by ACPD or PMA. (E) bar graph showing quantification of the data in *D* from multiple oocytes.

Moreover, these studies demonstrate trafficking and surface expression of homomeric KARs, whereas the modulation described here only occurs on heteromeric KARs with low- and high-affinity subunits and not homomeric KARs. Together with our study and that of Cho et al. (2003), the findings of Selak et al. (2009) make it likely that both mGlu-dependent facilitation and depression of KAR activity occurs at synapses. The potentiation described here occurs via a mechanism that involves modulation of the C terminus of the high-affinity KAR subunits. The endocytosis caused by PKC disruption of protein-protein interactions described by Selak et al. (2009) has a slower time course than the potentiation we describe here. In the current study, there appears to be a biphasic response of KAR currents after activation of mGlu receptors in which PKC-mediated potentiation of KAR activity is followed by a phosphatase-mediated decrease (Fig. 4B and Fig. 7, B and D). Therefore, we suggest that early facilitation, defacilitation (by phosphatase engagement), and subsequent

depression (via endocytosis) of GluK5-dependent activity may occur after group I mGlu and PKC activation. Additional experiments are necessary to pursue this idea and to determine the net functional consequences at different synapses.

Heteromeric KARs display unique functional properties. Exposure to DHPG and ACPD resulted in potentiation of the GluK2/GluK5 receptor AMPA steady-state currents in *X. laevis* oocytes when coexpressed with mGlu1 or mGlu5. However, bath application of ACPD failed to potentiate homomeric KARs expressed with mGlu1 and even inhibited GluK2 when expressed with mGlu5. In experiments involving *X. laevis* oocytes, activation of mGlu5 by ACPD or DHPG produced a lesser degree of heteromeric KAR potentiation, compared with activation of mGlu1 (Figs. 4C and 5), but a stronger degree of homomeric KAR inhibition (Fig. 4C). How can this occur? One possibility is that both mGlu1 and mGlu5 engage the $G\alpha_q$-Ca^{2+}–PLC-PKC pathway that potentiates heteromeric KAR, but that in addition, mGlu5 couples to an independent pathway that causes inhibition of both homomeric and heteromeric KAR. A potential mediator of this second pathway would be β-arrestin or a β-arrestin–like protein, which can act as a scaffolding molecule to bring selected G-protein coupled receptors into proximity with a variety of effector pathways (DeWire et al., 2007).

In the present study, key molecules in the mGlu1 s messenger cascade that are necessary for potentiation of GluK2/GluK5 were identified. Ultimately, the activities of these second messengers converge to activate PKC, which mediates potentiation of GluK2/GluK5 heteromers. The observed mGlu1-mediated potentiation of GluK2/GluK5 but not GluK2 strengthens the idea that the GluK5 subunit may be a regulatory subunit in the receptor complex. We identified a domain in the C terminus proximal to the third transmembrane domain of GluK5 that is critical for receptor potentiation. Our hypothesis that phosphorylation of this critical C-terminal domain of GluK5 is critically involved in potentiation was reinforced by mutation of potential phosphorylation sites. Alanine mutation of three GluK5 serines located in a membrane-proximal C-terminal domain rendered the receptor insensitive to mGlu1 activation. When these three serines were mutated to the phosphomimetic aspartate (GluK2/GluK5-S833D/S836D/S840D) and expressed with GluK2, significantly larger baseline currents were produced that were insensitive to PKC activation, as if this construct had been prepotentiated. These findings are consistent with the notion that overall electrostatic charge in this area is altered by phosphorylation of critical residues affecting the process of channel gating. However, negative charge on these residues alone is not sufficient for potentiation, because the triple glutamate mutant of GluK5 behaved like wild-type receptors. Of interest, the GluK5-TE-Δ884 mutant had normal baseline KAR currents but little to no regulation by mGlu1 and PMA, suggesting that additional phosphorylation sites that are normally inactive in the distal C terminus manifest themselves when the three critical serines are mutated to glutamate, which has a more flexible and larger side chain than does aspartate.

We were unable to resolve a clear mechanism explaining why heteromeric KARs behave differently than homomeric KARs. A disruption in the interaction between the high-affinity and low-affinity KARs could potentially explain the difference in modulation of heteromeric KARs and homomeric KARs by group I mGlu activation. Unfortunately, the interacting domains of the KAR subunits and the critical residues involved are not known. Additional experiments are necessary to address these ideas.

The importance of charged residues in this critical domain could potentially account for the lesser degree of potentiation of receptors containing GluK4, compared with GluK5, when combined with GluK2. A scan of the C terminus of GluK4 revealed that it also contains three serines (Ser834, Ser837, and Ser840) that are homologous to the three critical serines in GluK5. However, many of the other C-terminal residues and the overall length of the C termini are different between GluK4 and GluK5.

In conclusion, heteromeric KARs consisting of GluK2 and a high-affinity KAR subunit (GluK4 or GluK5) are potentiated by activation of group I mGlu receptors in a PKC-dependent manner, likely via phosphorylation of several critical residues located in the membrane-proximal C terminus of the GluK4 or GluK5. The regulation described here confers distinct functional properties to heteromeric KARs that may serve as one convergent molecular basis for control by group I mGlu receptors of KARs in synaptic plasticity and transmission.

Acknowledgments

The authors thank Nadia Lelutiu, Jamie Levin, and Stefanie Ritter (Emory University School of Medicine, Atlanta, GA) for their helpful technical discussions.

Authorship Contributions

Participated in research design: Rojas, Wetherington, Dingledine.

Conducted experiments: Rojas, Wetherington, Shaw, Serrano, Swanger.

Performed data analysis: Rojas, Wetherington, Dingledine.

Wrote or contributed to the writing of the manuscript: Rojas, Wetherington, Dingledine

References

Akiyama T, Ishida J, Nakagawa S, Ogawara H, Watanabe S, Itoh N, Shibuya M, and Fukami Y (1987) Genistein, a specific inhibitor of tyrosine-specific protein kinases. *J Biol Chem* **262**:5592–5595.

Alt A, Weiss B, Ogden AM, Knauss JL, Oler J, Ho K, Large TH, and Bleakman D (2004) Pharmacological characterization of glutamatergic agonists and antagonists at recombinant human homomeric and heteromeric kainate receptors in vitro. *Neuropharmacology* **46**:793–806.

Aniksztejn L, Otani S, and Ben-Ari Y (1992) Quisqualate Metabotropic Receptors Modulate NMDA Currents and Facilitate Induction of Long-Term Potentiation Through Protein Kinase C. *Eur J Neurosci* **4**:500–505.

Anwyl R (1994) Synaptic plasticity. A molecular switch for memory. *Curr Biol* **4**: 854–856.

Anwyl R (1999) Metabotropic glutamate receptors: electrophysiological properties and role in plasticity. *Brain Res Brain Res Rev* **29**:83–120.

Bahn S, Volk B, and Wisden W (1994) Kainate receptor gene expression in the developing rat brain. *J Neurosci* **14**:5525–5547.

Berthele A, Laurie DJ, Platzer S, Zieglgänsberger W, Tölle TR, and Sommer B (1998) Differential expression of rat and human type I metabotropic glutamate receptor splice variant messenger RNAs. *Neuroscience* **85**:733–749.

Besheer J and Hodge CW (2005) Pharmacological and anatomical evidence for an interaction between mGluR5- and GABA(A) alpha1-containing receptors in the discriminative stimulus effects of ethanol. *Neuropsychopharmacology* **30**:747–757.

Bettler B and Mulle C (1995) Review: neurotransmitter receptors. II. AMPA and kainate receptors. *Neuropharmacology* **34**:123–139.

Bortolotto ZA, Clarke VR, and Delany CM et al. (1999a) Kainate receptors are involved in synaptic plasticity. *Nature* **402**:297–301.

Bortolotto ZA, Fitzjohn SM, and Collingridge GL (1999b) Roles of metabotropic glutamate receptors in LTP and LTD in the hippocampus. *Curr Opin Neurobiol* **9**: 299–304.

Bureau I, Bischoff S, Heinemann SF, and Mulle C (1999) Kainate receptor-mediated responses in the CA1 field of wild-type and GluR6-deficient mice. *J Neurosci* **19**: 653–663.

Chamberlain SE, González-González IM, Wilkinson KA, Konopacki FA, Kantamneni S, Henley JM, and Mellor JR (2012) SUMOylation and phosphorylation of GluK2 regulate kainate receptor trafficking and synaptic plasticity. *Nat Neurosci* **15**: 845–852.

Chen C and Leonard JP (1996) Protein tyrosine kinase-mediated potentiation of currents from cloned NMDA receptors. *J Neurochem* **67**:194–200.
Chittajallu R, Vignes M, Dev KK, Barnes JM, Collingridge GL, and Henley JM (1996) Regulation of glutamate release by presynaptic kainate receptors in the hippocampus. *Nature* **379**:78–81.
Cho K, Francis JC, Hirbec H, Dev K, Brown MW, Henley JM, and Bashir ZI (2003) Regulation of kainate receptors by protein kinase C and metabotropic glutamate receptors. *J Physiol* **548**:723–730.
Clarke VR, Ballyk BA, and Hoo KH et al. (1997) A hippocampal GluR5 kainate receptor regulating inhibitory synaptic transmission. *Nature* **389**:599–603.
Darstein M, Petralia RS, Swanson GT, Wenthold RJ, and Heinemann SF (2003) Distribution of kainate receptor subunits at hippocampal mossy fiber synapses. *J Neurosci* **23**:8013–8019.
Dascal N (1997) Signalling via the G protein-activated K+ channels. *Cell Signal* **9**: 551–573.
DeWire SM, Ahn S, Lefkowitz RJ, and Shenoy SK (2007) Beta-arrestins and cell signaling. *Annu Rev Physiol* **69**:483–510.
Donevan SD, Beg A, Gunther JM, and Twyman RE (1998) The methylglutamate, SYM 2081, is a potent and highly selective agonist at kainate receptors. *J Pharmacol Exp Ther* **285**:539–545.
Egebjerg J and Heinemann SF (1993) Ca2+ permeability of unedited and edited versions of the kainate selective glutamate receptor GluR6. *Proc Natl Acad Sci USA* **90**:755–759.
Ferraguti F, Conquet F, Corti C, Grandes P, Kuhn R, and Knopfel T (1998) Immunohistochemical localization of the mGluR1beta metabotropic glutamate receptor in the adult rodent forebrain: evidence for a differential distribution of mGluR1 splice variants. *J Comp Neurol* **400**:391–407.
Geissler JF, Traxler P, Regenass U, Murray BJ, Roesel JL, Meyer T, McGlynn E, Storni A, and Lydon NB (1990) Thiazolidine-diones. Biochemical and biological activity of a novel class of tyrosine protein kinase inhibitors. *J Biol Chem* **265**: 22255–22261.
Harvey J and Collingridge GL (1993) Signal transduction pathways involved in the acute potentiation of NMDA responses by 1S,3R-ACPD in rat hippocampal slices. *Br J Pharmacol* **109**:1085–1090.
Hirbec H, Francis JC, and Lauri SE et al. (2003) Rapid and differential regulation of AMPA and kainate receptors at hippocampal mossy fibre synapses by PICK1 and GRIP. *Neuron* **37**:625–638.
Huettner JE (2003) Kainate receptors and synaptic transmission. *Prog Neurobiol* **70**: 387–407.
Isaac JT, Mellor J, Hurtado D, and Roche KW (2004) Kainate receptor trafficking: physiological roles and molecular mechanisms. *Pharmacol Ther* **104**:163–172.
Jiang J, Ganesh T, and Du Y et al. (2010) Neuroprotection by selective allosteric potentiators of the EP2 prostaglandin receptor. *Proc Natl Acad Sci USA* **107**: 2307–2312.
Kawajiri S and Dingledine R (1993) Multiple structural determinants of voltage-dependent magnesium block in recombinant NMDA receptors. *Neuropharmacology* **32**:1203–1211.
Kelso SR, Nelson TE, and Leonard JP (1992) Protein kinase C-mediated enhancement of NMDA currents by metabotropic glutamate receptors in Xenopus oocytes. *J Physiol* **449**:705–718.
Kleckner NW and Dingledine R (1988) Requirement for glycine in activation of NMDA-receptors expressed in Xenopus oocytes. *Science* **241**:835–837.
Köhr G and Seeburg PH (1996) Subtype-specific regulation of recombinant NMDA receptor-channels by protein tyrosine kinases of the src family. *J Physiol* **492**: 445–452.
Konopacki FA, Jaafari N, Rocca DL, Wilkinson KA, Chamberlain S, Rubin P, Kantamneni S, Mellor JR, and Henley JM (2011) Agonist-induced PKC phosphorylation regulates GluK2 SUMOylation and kainate receptor endocytosis. *Proc Natl Acad Sci USA* **108**:19772–19777.
Kornreich BG, Niu L, Roberson MS, and Oswald RE (2007) Identification of C-terminal domain residues involved in protein kinase A-mediated potentiation of kainate receptor subtype 6. *Neuroscience* **146**:1158–1168.
Lerma J (2003) Roles and rules of kainate receptors in synaptic transmission. *Nat Rev Neurosci* **4**:481–495.
Lerma J, Paternain AV, Rodríguez-Moreno A, and López-García JC (2001) Molecular physiology of kainate receptors. *Physiol Rev* **81**:971–998.
Manders EMM, Verbeek FJ, and Aten JA (1993) Measurement of Colocalization of Objects in Dual-Color Confocal Images. *Journal of Microscopy* **169**:375–382.
Mott DD, Benveniste M, and Dingledine RJ (2008) pH-dependent inhibition of kainate receptors by zinc. *J Neurosci* **28**:1659–1671.
Mott DD, Rojas A, Fisher JL, Dingledine RJ, and Benveniste M (2010) Subunit-specific desensitization of heteromeric kainate receptors. *J Physiol* **588**:683–700.
Nasu-Nishimura Y, Jaffe H, Isaac JT, and Roche KW (2010) Differential regulation of kainate receptor trafficking by phosphorylation of distinct sites on GluR6. *J Biol Chem* **285**:2847–2856.
Paternain AV, Herrera MT, Nieto MA, and Lerma J (2000) GluR5 and GluR6 kainate receptor subunits coexist in hippocampal neurons and coassemble to form functional receptors. *J Neurosci* **20**:196–205.
Raymond LA, Blackstone CD, and Huganir RL (1993) Phosphorylation and modulation of recombinant GluR6 glutamate receptors by cAMP-dependent protein kinase. *Nature* **361**:637–641.
Raymond LA, Tingley WG, Blackstone CD, Roche KW, and Huganir RL (1994) Glutamate receptor modulation by protein phosphorylation. *J Physiol Paris* **88**: 181–192.
Rivera R, Rozas JL, and Lerma J (2007) PKC-dependent autoregulation of membrane kainate receptors. *EMBO J* **26**:4359–4367.
Rodríguez-Moreno A, Herreras O, and Lerma J (1997) Kainate receptors presynaptically downregulate GABAergic inhibition in the rat hippocampus. *Neuron* **19**:893–901.
Ruiz A, Sachidhanandam S, Utvik JK, Coussen F, and Mulle C (2005) Distinct subunits in heteromeric kainate receptors mediate ionotropic and metabotropic function at hippocampal mossy fiber synapses. *J Neurosci* **25**:11710–11718.
Schiffer HH, Swanson GT, and Heinemann SF (1997) Rat GluR7 and a carboxy-terminal splice variant, GluR7b, are functional kainate receptor subunits with a low sensitivity to glutamate. *Neuron* **19**:1141–1146.
Selak S, Paternain AV, Aller MI, Picó E, Rivera R, and Lerma J (2009) A role for SNAP25 in internalization of kainate receptors and synaptic plasticity. *Neuron* **63**: 357–371.
Simonyi A, Ngomba RT, Storto M, Catania MV, Miller LA, Youngs B, DiGiorgi-Gerevini V, Nicoletti F, and Sun GY (2005) Expression of groups I and II metabotropic glutamate receptors in the rat brain during aging. *Brain Res* **1043**: 95–106.
Sommer B, Burnashev N, Verdoorn TA, Keinänen K, Sakmann B, and Seeburg PH (1992) A glutamate receptor channel with high affinity for domoate and kainate. *EMBO J* **11**:1651–1656.
Traynelis SF and Wahl P (1997) Control of rat GluR6 glutamate receptor open probability by protein kinase A and calcineurin. *J Physiol* **503**:513–531.
Traynelis SF, Wollmuth LP, McBain CJ, Menniti FS, Vance KM, Ogden KK, Hansen KB, Yuan H, Myers SJ, and Dingledine R (2010) Glutamate receptor ion channels: structure, regulation, and function. *Pharmacol Rev* **62**:405–496.
Wang LY, Taverna FA, Huang XP, MacDonald JF, and Hampson DR (1993) Phosphorylation and modulation of a kainate receptor (GluR6) by cAMP-dependent protein kinase. *Science* **259**:1173–1175.
Wang YT and Salter MW (1994) Regulation of NMDA receptors by tyrosine kinases and phosphatases. *Nature* **369**:233–235.
Wenthold RJ, Trumpy VA, Zhu WS, and Petralia RS (1994) Biochemical and assembly properties of GluR6 and KA2, two members of the kainate receptor family, determined with subunit-specific antibodies. *J Biol Chem* **269**:1332–1339.

Address correspondence to: Dr. Asheebo Rojas, Department of Pharmacology, Emory University School of Medicine, 1510 Clifton Road, Atlanta, GA 30322. E-mail: arojas@pharm.emory.edu